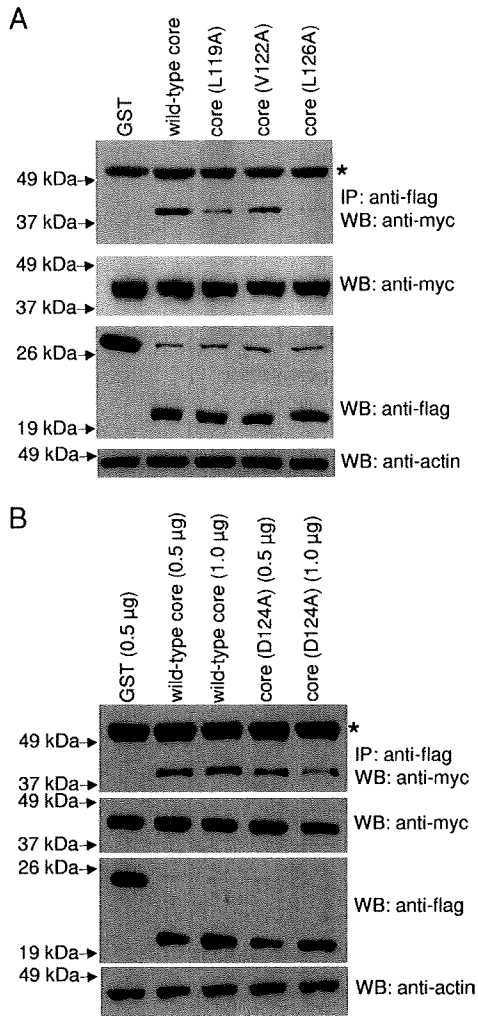

FIG. 7. Effects of alanine substitutions on the binding of the core protein to Mcl-1. (A) Huh7 cells were transfected with cDNA constructs (1.0 μg) for expressing flag-GST (negative control), flag-tagged wild-type core protein, or single-alanine-substitution mutants (L119A, V122A, and L126A). All cells were cotransfected with myc-tagged Mcl-1 (1.5 μg). (B) Huh7 cells were transfected with cDNA constructs for expressing flag-GST (negative control, 0.5 μg), flag-tagged wild-type core protein (0.5 or 1.0 μg), or single-alanine-substitution mutant D124A (0.5 or 1.0 μg). All cells were cotransfected with myc-tagged Mcl-1 (1.5 μg). Coimmunoprecipitation then was performed as described in the legend to Fig. 3A. The amount of myc-tagged proteins that coimmunoprecipitated (IP) with the flag-tagged proteins was determined by Western blot analysis (WB) with an anti-myc rabbit polyclonal antibody (top). The amounts of myc-tagged and flag-tagged proteins in the lysates before IP were determined by subjecting aliquots of the lysates to Western blot analysis (middle). The amounts of total cell lysates loaded were verified by measuring the levels of endogenous actin (bottom). The protein marked with an asterisk represents the heavy chain of the antibody used for IP (top). Similar results were obtained in four independent experiments, and a representative set of data is presented.

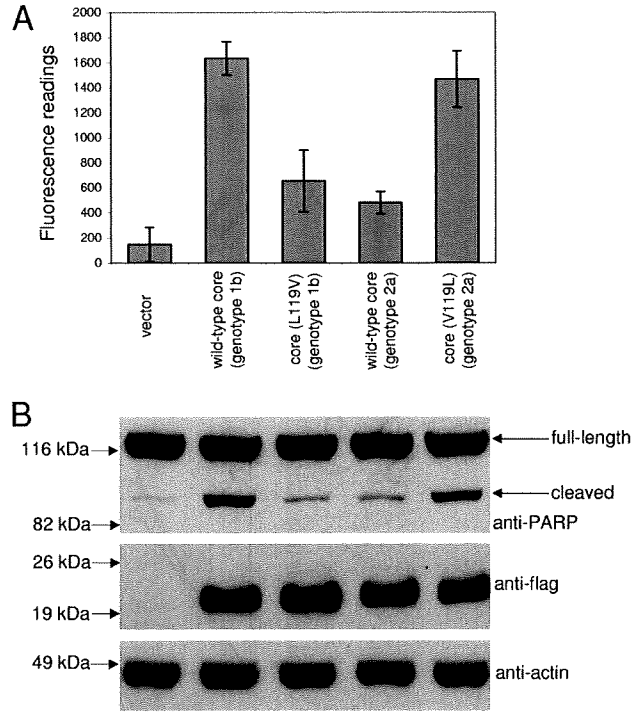

FIG. 8. Comparison of the proapoptotic properties of the core proteins of genotypes 1b and 2a. (A) A CaspACE fluorometric assay system from Promega Corporation (Madison, WI) was used to measure the activation of caspase-3 in Huh7 cells that were transfected with vector only, wild-type core of genotype 1b or 2a, or their substitution mutants. All experiments were performed in triplicate, and the average values with standard deviations are plotted. (B) Western blot analysis also was performed to determine the cleavage of endogenous PARP (top) and expression levels of the core proteins (middle). The amounts of total cell lysates loaded were verified by measuring the levels of endogenous actin (bottom).

vival members vary greatly (11, 32). For example, Bim and Puma bind all prosurvival members tested, while Noxa binds strongly only to Mcl-1 and A1. On the other hand, Bad binds much more strongly to Bcl-2, Bcl-X_L, and Bcl-w than Mcl-1. Taken together with results from successive studies, it becomes clear that the BH3-only members can be classified into subclasses (see reviews in references 21, 24, 58, and 71). In this study, we demonstrate that the HCV core protein is a BH3-only viral homologue of the Bcl-2 family, and its BH3 domain is essential for the induction of apoptosis (Fig. 1 and 2). In coimmunoprecipitation experiments, the core protein interacted specifically with the prosurvival Mcl-1 protein but not with prosurvival proteins Bcl-X_L and Bcl-w (Fig. 3), suggesting that its property is most similar to that of Noxa (11). Consistently, the overexpression of Mcl-1 protects against core protein-induced apoptosis (Fig. 4). However, the overexpression of Bcl-X_L also protects against core protein-induced apoptosis (Fig. 4). This may be due to the ability of a high level of Bcl-X_L to prevent the complementation between the core protein and endogenous Bad protein, which binds strongly to Bcl-X_L (11), as we have observed that a combination of the core protein and Bad peptide mimetics caused efficient cytochrome *c* release from the mitochondria (Fig. 5). The complementation between Bad and the core protein is similar to that observed between Bad and Noxa, which act in combination to neutralize the two classes of prosurvival proteins, one comprised of Bcl-2, Bcl-X_L, and Bcl-w and the other of Mcl-1 and A1 (11). In overexpres-

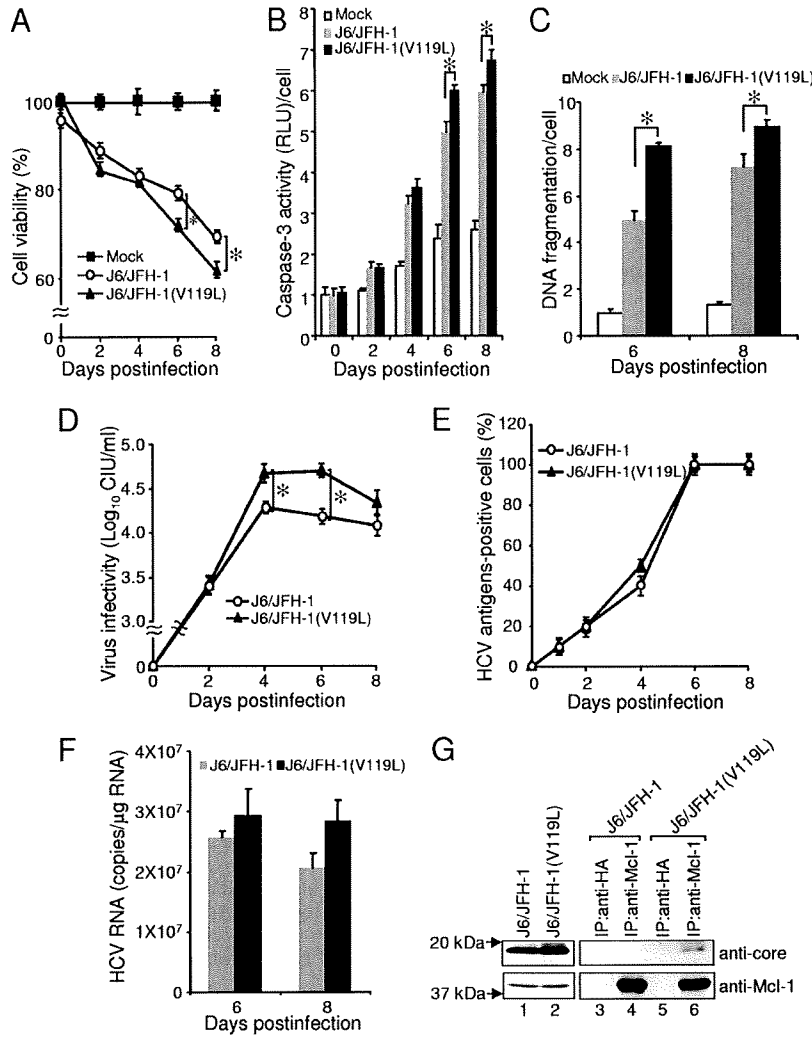

FIG. 9. Comparison of parental J6/JFH-1 and mutant J6/JFH-1(V119L) recombinant viruses. Huh7.5 cells were infected with recombinant HCV at a multiplicity of infection of 0.1 CIU/cell or with a mock preparation, and various assays were performed at different days after infection. (A) Cell viabilities were determined. (B) Caspase-3 activity per cell was determined. (C) The amount of DNA fragmentation per cell was determined. (D) The production of cell-free infectious virus particles was determined. (E) Virus spread in the culture was quantitated. (F) HCV RNA replication was determined by quantitative real-time PCR analysis. (G) Interaction of the core protein with Mcl-1 was determined by coimmunoprecipitation experiments at 3 days p.i. IP was performed using anti-Mcl-1 or anti-HA rabbit polyclonal antibodies and protein A agarose beads. The amounts of the core protein in the lysates before (lanes 1 and 2) and after IP (lanes 3 to 6) were determined by Western blot analysis with an anti-core monoclonal antibody (top). Similarly, the amounts of endogenous Mcl-1 in the samples were determined using an anti-Mcl-1 monoclonal antibody (bottom). Statistical analysis was performed using the one-way analysis of variance to determine if the differences between parental and mutant viruses were statistically significant, and those with P values of <0.05 (marked by asterisks) are considered statistically significant. Data were obtained from three independent experiments, each with triplicate cultures.

sion studies, the core protein and Noxa also induced comparable levels of apoptosis (see Fig. S3 and S5 in the supplemental material). Taken together, these findings suggest that core can mimic Noxa and interfere directly with the prosurvival function of Mcl-1.

A comparison of the BH3 domain of the core protein to the corresponding domains of other BH3-containing proteins (Fig. 1A) revealed that it contains three out of the four hydrophobic residues that can be accommodated within the hydrophobic pockets of previously described BH3 binding grooves (see reviews in references 50 and 69). Alanine substitution experiments revealed that all three hydrophobic residues in the BH3 domain of the core protein are essential for apoptosis induction (Fig. 6). In coimmunoprecipitation experiments, these alanine substitution mutants also bound Mcl-1 to a lesser extent than the wild-type core protein (Fig. 7A). Since these alanine substitution mutants still can bind Mcl-1, albeit at a lower level than that of the wild-type core protein, it appears that the interactions between these mutants and Mcl-1 are not sufficient to induce apoptosis. In several mutagenesis studies, the interaction between Bcl-2 family members and apoptosis regulation have been observed to be discordant. For example, two mutants of the BH3-only protein Bik, Bik-(43-94) and Bik-(43-120), heterodimerized with prosurvival Bcl-2 and Bcl-X_L but

were unable to induce efficient cell death (19). A Bad mutant containing an alteration of a critical residue within its BH3 domain, E113 to K, also was found to have significantly reduced apoptotic activity compared to that of wild-type Bad, despite binding to Bcl-2 and/or Bcl-X_L to the same extent as wild-type Bad (35). Therefore, the induction of apoptosis by the core protein may be controlled by a critical threshold affinity of binding between the core protein and Mcl-1, or there are contributions from a yet-to-be characterized pathway(s). Two of these residues (V122 and L126) are conserved in the major genotypes of HCV, but residue 119 is a V in genotype 2a (Fig. 1B). When L119 of the genotype 1b core protein was replaced with V, its ability to induce apoptosis was greatly reduced (Fig. 8). Conversely, when V119 of the genotype 2a core protein was replaced with L, its ability to induce apoptosis was greatly enhanced. Thus, the results suggest that the genotype 1b core protein induces apoptosis efficiently via a BH3 domain, while genotype 2a core protein is comparatively less efficient. Another highly conserved residue in the BH3 domain of the core protein is D124. However, the replacement of D124 with A did not reduce the proapoptotic function of the core protein (Fig. 6). Thus far, there are only a few known functional BH3 domains that do not contain D at this position (61, 62). Unlike most BH3-only proteins, the core protein has a charged residue (R115) in the h1 position (Fig. 1A). Interestingly, the second BH3 domain of mouse Noxa (mNoxaB) also has a charged residue (E74) in this position. Indeed, the nuclear magnetic resonance structure of the complex between mouse Mcl-1 and a peptide mimetic of mNoxaB shows that E74 is tolerated at the h1 position because its charged carboxyl group is coordinated by another charged residue, K215, in mouse Mcl-1 (15). However, R115 of the core protein is basic instead of acidic, and how this residue can be accommodated in the hydrophobic groove of Mcl-1 is unclear. Interestingly, replacing the residue at the h1 position (I58) of a novel BimBH3 variant, Bim_S2A, with A also has little effect on its interaction with Mcl-1 (34). Thus, it appears that the residue in the h1 position is not always involved in the interaction between BH3-only proteins and Mcl-1, but further biophysical and biochemical studies are required to delineate the precise structure-function relationship for the interaction between core and Mcl-1.

To determine if the results from overexpression studies are relevant to the modulation of apoptosis in host cells during HCV infection, the J6/JFH-1-based (genotype 2a) system was used to generate HCV carrying a substitution at residue 119 of the core protein. While the parental wild-type and mutant viruses replicated efficiently in Huh7.5 cells, the J6/JFH-1(V119L) virus (which expresses the core protein with L at the h2 position of the BH3 domain) caused a significantly higher level of apoptosis in the infected cells than the parental J6/JFH-1 virus (which expresses the core protein with V at the h2 position of the BH3 domain) (Fig. 9). This is in good agreement with the overexpression studies and indicates that the BH3 domain of the core protein contributes to the induction of apoptosis in HCV-infected cells. Thus, it appears that core protein-mediated apoptosis during infection by HCV of genotype 2a is less efficient than that of the other genotypes having L at residue 119 of the core protein (Fig. 1B). Coimmunoprecipitation experiments revealed that the core protein of J6/JFH-1(V119L), but not that of J6/JFH-1, interacted with Mcl-1 in virus-infected cells (Fig. 9). This result is consistent with the overexpression studies and suggests the possibility that the core protein induces apoptosis, at least partly, through the interaction with Mcl-1 in HCV-infected cells. Interestingly, more progeny virus is released from cells infected with the J6/JFH-1(V119L) virus than by those infected with the parental J6/JFH-1, while there is no difference in the efficiency of infection or amount of HCV replication inside the cells (Fig. 9).

However, it also is apparent that the parental J6/JFH-1 virus still caused a high level of apoptosis in the infected cells, and for the early time points there was no significant difference in the levels of apoptosis induced by the parental J6/JFH-1 virus and the J6/JFH-1(V119L) mutant virus (Fig. 9). This implies that there are other viral factors that contribute to the induction of apoptosis during HCV infection. For example, several nonstructural HCV proteins, like NS3, NS4A, NS5A, and NS5B, can induce apoptosis when they are overexpressed in certain types of cells (see recent reviews in references 20 and 28). In addition, other domains in the core protein have been shown to bind host proteins and may contribute to apoptosis regulation by interfering with different cellular pathways (see reviews in references 33, 42, and 52). For example, the N-terminal domain (aa 1 to 75) of the core protein interacts with Hsp60, leading to the production of reactive oxygen species and enhancement of tumor necrosis factor alpha-mediated apoptosis (30), while a C-terminal domain (aa 153 to 192) facilitates Fas oligomerization and is required for apoptosis induction in Jurkat cells (46). However, the relative contribution of these various factors to apoptosis induction during HCV infection remains to be determined.

We further examined the importance of residue 119 of the core protein in HCV replication. In multiple independent transfection experiments, we observed that the J6/JFH-1 mutant possessing A at position 119 [J6/JFH-1(V119A)] barely replicated in the cells and did not produce any infectious virus particles in the culture supernatants (data not shown). This result suggests the possibility that this single point mutation impairs the interaction of the core protein with other viral and/or cellular protein(s) that is required for HCV RNA replication and infectious virion production. Similarly, the J6/JFH-1 mutants each possessing A at positions 122 [J6/JFH-1(V122A)], 124 [J6/JFH-1(D124A)], or 126 [J6/JFH-1(L126A)] barely replicated in the cells and did not produce any infectious virion in the culture supernatants (data not shown), with the results suggesting an important role(s) for these residues as well as for position 119. In this connection, the essential role for the HCV core protein in infectious virion production recently has been confirmed, and numerous residues required for this role have been identified (47).

By using the JFH-1 infectious clone, recent studies have revealed that the association of the core protein with the lipid droplet (LD) is critical for the production of infectious virus particles (6, 45). Boulant and coworkers reported that there are two amphipathic α-helices in the so-called D2 domain of the core protein (~118 to 179 aa) (5, 7), and the hydrophobic residues within this domain are critical for the efficient attachment of the core protein to LD (5). Our results showed that residues L119, V122, and L126 of the core protein are essential

for the induction of apoptosis, and these residues are found on the hydrophobic face of the first α-helix of the D2 domain. Interestingly, the replacement of L119 with E did not affect LD association, while the replacement of L126 with E significantly reduced LD association (5). The contribution of V122 to LD association was not investigated. Consistently, the J6/JFH-1(V119L) virus, but not the J6/JFH-1(L126A) virus, replicated efficiently to produce infectious virus particles. Since L119 of the genotype 1b core protein, which occupies the crucial h2 position in the BH3 domain, is essential for its proapoptotic property but not for its association with LD, it is clear that the BH3 domain of the core protein is an independent motif that partially overlaps with the LD association domain.

Recently, Makes caterpillars floppy 1 (Mcf1), a bacterial toxin, was reported to contain a BH3-like domain (18). In addition, HBSP, a spliced hepatitis B viral protein, also contains a BH3-like domain (39). Here, we show that the HCV core protein is another BH3-like viral homologue, and it contributes directly to the induction of apoptosis during HCV infection. Our results also reveal that it is a bona fide BH3-only protein that appears to interfere with the prosurvival property of Mcl-1 in a manner similar to that of Noxa. Our observation that the enhanced apoptotic activity of the J6/JFH-1(V119L) virus is correlated with an increase in infectious progeny HCV release seems to be counterintuitive, as many viruses adopted strategies to prevent apoptosis in the infected cells so as to allow viral replication and the packaging of progeny genomes within the cells (14, 26, 51, 70). However, enhanced releases of virus from infected cells that are undergoing apoptosis also have been reported for other viruses, like the infectious bursal disease virus, adenovirus, and Aleutian mink disease parvovirus (4, 44, 73), indicating that apoptosis can be advantageous for viral spreading at the late stages of infection. Future studies to define the precise manner by which the BH3 domain of the core protein modulates apoptosis during infection will provide important insights into HCV replication as well as pathogenesis.

Besides the genotype 1b core protein, the properties of the genotype 1a core protein also have been examined in various studies. The apoptotic property of the genotype 1a core protein has yet to be studied using the JFH-1-based infectious clone system, although previous studies have attributed both prosurvival and proapoptotic properties to it (25, 30, 46, 57). Similar observations also have been described in overexpression studies using the genotype 1b core protein and appear to be dependent on the death stimuli and types of cells used (3, 9, 10, 36, 49, 53, 56, 60, 76). Several studies have identified domains or regions within the core protein that interfere with specific apoptosis pathways. For instance, the interaction of the N-terminal domain (residues 1 to 75) of the genotype 1a core protein with Hsp60 enhanced tumor necrosis factor alpha-mediated apoptosis, while its C-terminal region (residues 153 to 192) is required for Fas ligand-independent apoptosis (30, 46). The genotype 1b core protein (residues 1 to 153) binds to the death domain of FADD, resulting in enhanced apoptosis (76). However, an overlapping domain spanning the first 46 aa of the core protein is involved in ASPP2 interaction, which leads to the inhibition of p53-mediated apoptosis (9). These findings suggest that multiple domains present in the core protein contribute to the modulation of apoptosis via diverse pathways. Therefore, the net apoptotic effect of the core protein may be dependent on the relative strength of its prosurvival and proapoptotic properties. Unlike the genotype 2a core protein, the BH3 domains of the genotype 1b core protein and the genotype 1a core protein share an identical sequence (Fig. 1B) and are expected to function in a similar manner. However, we cannot rule out that there may be differences in the manner in which the core proteins of genotypes 1a and 1b modulate apoptosis during infection. For example, they may be involved in different virus-virus or virus-host interactions. Thus, more studies are needed to understand the contributions of genotype-dependent factors to the regulation of apoptosis during HCV infection.

ACKNOWLEDGMENTS

We thank T. Wakita for the JFH-1 construct and anti-core monoclonal antibody and C. M. Rice for the J6/JFH-1 construct and Huh7.5 cells.

This work was supported by the Biomedical Research Council of A*STAR (Agency for Science, Technology and Research), Singapore, a Health and Labor Sciences Research Grant from the Ministry of Health, Labor and Welfare, Japan, and the Program of Founding Research Centers for Emerging and Reemerging Infectious Diseases, the Ministry of Education, Culture, Sports, Science and Technology, Japan.

Y.-J.T. is an adjunct staff member of the Department of Microbiology at the National University of Singapore.

REFERENCES

1. **Adams, J. M., and S. Cory.** 2007. Bcl-2-regulated apoptosis: mechanism and therapeutic potential. Curr. Opin. Immunol. **19**:488–496.
2. **Bartenschlager, R., and V. Lohmann.** 2000. Replication of hepatitis C virus. J. Gen. Virol. **81**:1631–1648.
3. **Benali-Furet, N. L., M. Chami, L. Houel, F. De Giorgi, F. Vernejoul, D. Lagorce, L. Buscail, R. Bartenschlager, F. Ichas, R. Rizzuto, and P. Paterlini-Brechot.** 2005. Hepatitis C virus core triggers apoptosis in liver cells by inducing ER stress and ER calcium depletion. Oncogene **24**:4921–4933.
4. **Best, S. M., J. B. Wolfinbarger, and M. E. Bloom.** 2002. Caspase activation is required for permissive replication of Aleutian mink disease parvovirus in vitro. Virology **292**:224–234.
5. **Boulant, S., R. Montserret, R. G. Hope, M. Ratinier, P. Targett-Adams, J. P. Lavergne, F. Penin, and J. McLauchlan.** 2006. Structural determinants that target the hepatitis C virus core protein to lipid droplets. J. Biol. Chem. **281**:22236–22247.
6. **Boulant, S., P. Targett-Adams, and J. McLauchlan.** 2007. Disrupting the association of hepatitis C virus core protein with lipid droplets correlates with a loss in production of infectious virus. J. Gen. Virol. **88**:2204–2213.
7. **Boulant, S., C. Vanbelle, C. Ebel, F. Penin, and J. P. Lavergne.** 2005. Hepatitis C virus core protein is a dimeric alpha-helical protein exhibiting membrane protein features. J. Virol. **79**:11353–11365.
8. **Boya, P., A. L. Pauleau, D. Poncet, R. A. Gonzalez-Polo, N. Zamzami, and G. Kroemer.** 2004. Viral proteins targeting mitochondria: controlling cell death. Biochim. Biophys. Acta **1659**:178–189.
9. **Cao, Y., T. Hamada, T. Matsui, T. Date, and K. Iwabuchi.** 2004. Hepatitis C virus core protein interacts with p53-binding protein, 53BP2/Bbp/ASPP2, and inhibits p53-mediated apoptosis. Biochem. Biophys. Res. Commun. **315**:788–795.
10. **Chang, M. L., J. C. Chen, M. Y. Chang, C. T. Yeh, W. P. Lin, C. K. Liang, S. F. Huang, K. N. Dang, C. T. Chiu, and D. Y. Lin.** 2008. Acute expression of hepatitis C core protein in adult mouse liver: mitochondrial stress and apoptosis. Scand. J. Gastroenterol. **43**:747–755.
11. **Chen, L., S. N. Willis, A. Wei, B. J. Smith, J. I. Fletcher, M. G. Hinds, P. M. Colman, C. L. Day, J. M. Adams, and D. C. Huang.** 2005. Differential targeting of prosurvival Bcl-2 proteins by their BH3-only ligands allows complementary apoptotic function. Mol. Cell **17**:393–403.
12. **Cheng, E. H., D. G. Kirsch, R. J. Clem, R. Ravi, M. B. Kastan, A. Bedi, K. Ueno, and J. M. Hardwick.** 1997. Conversion of Bcl-2 to a Bax-like death effector by caspases. Science **278**:1966–1968.
13. **Chou, A. H., H. F. Tsai, Y. Y. Wu, C. Y. Hu, L. H. Hwang, P. I. Hsu, and P. N. Hsu.** 2005. Hepatitis C virus core protein modulates TRAIL-mediated apoptosis by enhancing Bid cleavage and activation of mitochondria apoptosis signaling pathway. J. Immunol. **174**:2160–2166.
14. **Cuconati, A., and E. White.** 2002. Viral homologs of BCL-2: role of apoptosis in the regulation of virus infection. Genes Dev. **16**:2465–2478.

15. **Czabotar, P. E., E. F. Lee, M. F. van Delft, C. L. Day, B. J. Smith, D. C. Huang, W. D. Fairlie, M. G. Hinds, and P. M. Colman.** 2007. Structural insights into the degradation of Mcl-1 induced by BH3 domains. Proc. Natl. Acad. Sci. USA **104**:6217–6222.
16. **Danial, N. N.** 2007. BCL-2 family proteins: critical checkpoints of apoptotic cell death. Clin. Cancer Res. **13**:7254–7263.
17. **Deng, L., T. Adachi, K. Kitayama, Y. Bungyoku, S. Kitazawa, S. Ishido, I. Shoji, and H. Hotta.** 2008. Hepatitis C virus infection induces apoptosis through a Bax-triggered, mitochondria-mediated, caspase-3-dependent pathway. J. Virol. **82**:10375–10385.
18. **Dowling, A. J., N. R. Waterfield, M. C. Hares, G. Le Goff, C. H. Streuli, and R. H. ffrench-Constant.** 2007. The Mcf1 toxin induces apoptosis via the mitochondrial pathway and apoptosis is attenuated by mutation of the BH3-like domain. Cell Microbiol. **9**:2470–2484.
19. **Elangovan, B., and G. Chinnadurai.** 1997. Functional dissection of the pro-apoptotic protein Bik. Heterodimerization with anti-apoptosis proteins is insufficient for induction of cell death. J. Biol. Chem. **272**:24494–24498.
20. **Fischer, R., T. Baumert, and H. E. Blum.** 2007. Hepatitis C virus infection and apoptosis. World J. Gastroenterol. **13**:4865–4872.
21. **Fletcher, J. I., and D. C. Huang.** 2008. Controlling the cell death mediators Bax and Bak: puzzles and conundrums. Cell Cycle **7**:39–44.
22. **Fu, N. Y., S. K. Sukumaran, and V. C. Yu.** 2007. Inhibition of ubiquitin-mediated degradation of MOAP-1 by apoptotic stimuli promotes Bax function in mitochondria. Proc. Natl. Acad. Sci. USA **104**:10051–10056.
23. **Galluzzi, L., C. Brenner, E. Morselli, Z. Touat, and G. Kroemer.** 2008. Viral control of mitochondrial apoptosis. PLoS Pathog. **4**:e1000018.
24. **Häcker, G., and A. Weber.** 2007. BH3-only proteins trigger cytochrome *c* release, but how? Arch. Biochem. Biophys. **462**:150–155.
25. **Hahn, C. S., Y. G. Cho, B. S. Kang, I. M. Lester, and Y. S. Hahn.** 2000. The HCV core protein acts as a positive regulator of fas-mediated apoptosis in a human lymphoblastoid T cell line. Virology **276**:127–137.
26. **Hardwick, J. M., and D. S. Bellows.** 2003. Viral versus cellular BCL-2 proteins. Cell Death Differ. **10**(Suppl. 1):S68–S76.
27. **Hay, S., and G. Kannourakis.** 2002. A time to kill: viral manipulation of the cell death program. J. Gen. Virol. **83**:1547–1564.
28. **Herzer, K., M. F. Sprinzl, and P. R. Galle.** 2007. Hepatitis viruses: live and let die. Liver Int. **27**:293–301.
29. **Hope, R. G., and J. McLauchlan.** 2000. Sequence motifs required for lipid droplet association and protein stability are unique to the hepatitis C virus core protein. J. Gen. Virol. **81**:1913–1925.
30. **Kang, S. M., S. J. Kim, J. H. Kim, W. Lee, G. W. Kim, K. H. Lee, K. Y. Choi, and J. W. Oh.** 2009. Interaction of hepatitis C virus core protein with Hsp60 triggers the production of reactive oxygen species and enhances TNF-alpha-mediated apoptosis. Cancer Lett. **279**:230–237.
31. **Kozopas, K. M., T. Yang, H. L. Buchan, P. Zhou, and R. W. Craig.** 1993. MCL1, a gene expressed in programmed myeloid cell differentiation, has sequence similarity to BCL2. Proc. Natl. Acad. Sci. USA **90**:3516–3520.
32. **Kuwana, T., L. Bouchier-Hayes, J. E. Chipuk, C. Bonzon, B. A. Sullivan, D. R. Green, and D. D. Newmeyer.** 2005. BH3 domains of BH3-only proteins differentially regulate Bax-mediated mitochondrial membrane permeabilization both directly and indirectly. Mol. Cell **17**:525–535.
33. **Lai, M. M., and C. F. Ware.** 2000. Hepatitis C virus core protein: possible roles in viral pathogenesis. Curr. Top. Microbiol. Immunol. **242**:117–134.
34. **Lee, E. F., P. E. Czabotar, M. F. van Delft, E. M. Michalak, M. J. Boyle, S. N. Willis, H. Puthalakath, P. Bouillet, P. M. Colman, D. C. Huang, and W. D. Fairlie.** 2008. A novel BH3 ligand that selectively targets Mcl-1 reveals that apoptosis can proceed without Mcl-1 degradation. J. Cell Biol. **180**:341–355.
35. **Lee, J. W., Y. H. Soung, S. Y. Kim, S. W. Nam, C. J. Kim, Y. G. Cho, J. H. Lee, H. S. Kim, W. S. Park, S. H. Kim, J. Y. Lee, N. J. Yoo, and S. H. Lee.** 2004. Inactivating mutations of proapoptotic Bad gene in human colon cancers. Carcinogenesis **25**:1371–1376.
36. **Lee, S. K., S. O. Park, C. O. Joe, and Y. S. Kim.** 2007. Interaction of HCV core protein with 14-3-3epsilon protein releases Bax to activate apoptosis. Biochem. Biophys. Res. Commun. **352**:756–762.
37. **Lindenbach, B. D., M. J. Evans, A. J. Syder, B. Wolk, T. L. Tellinghuisen, C. C. Liu, T. Maruyama, R. O. Hynes, D. R. Burton, J. A. McKeating, and C. M. Rice.** 2005. Complete replication of hepatitis C virus in cell culture. Science **309**:623–626.
38. **Liu, Q., C. Tackney, R. A. Bhat, A. M. Prince, and P. Zhang.** 1997. Regulated processing of hepatitis C virus core protein is linked to subcellular localization. J. Virol. **71**:657–662.
39. **Lu, Y. W., T. L. Tan, V. Chan, and W. N. Chen.** 2006. The HBSP gene is expressed during HBV replication, and its coded BH3-containing spliced viral protein induces apoptosis in HepG2 cells. Biochem. Biophys. Res. Commun. **351**:64–70.
40. **Marusawa, H., M. Hijikata, T. Chiba, and K. Shimotohno.** 1999. Hepatitis C virus core protein inhibits Fas- and tumor necrosis factor alpha-mediated apoptosis via NF-κB activation. J. Virol. **73**:4713–4720.
41. **Mateu, G., R. O. Donis, T. Wakita, J. Bukh, and A. Grakoui.** 2008. Intragenotypic JFH1 based recombinant hepatitis C virus produces high levels of infectious particles but causes increased cell death. Virology **376**:397–407.
42. **McLauchlan, J.** 2000. Properties of the hepatitis C virus core protein: a structural protein that modulates cellular processes. J. Viral Hepat. **7**:2–14.
43. **McLean, J. E., A. Ruck, A. Shirazian, F. Pooyaei-Mehr, and Z. F. Zakeri.** 2008. Viral manipulation of cell death. Curr. Pharm. Des. **14**:198–220.
44. **Mi, J., Z. Y. Li, S. Ni, D. Steinwaerder, and A. Lieber.** 2001. Induced apoptosis supports spread of adenovirus vectors in tumors. Hum. Gene Ther. **12**:1343–1352.
45. **Miyanari, Y., K. Atsuzawa, N. Usuda, K. Watashi, T. Hishiki, M. Zayas, R. Bartenschlager, T. Wakita, M. Hijikata, and K. Shimotohno.** 2007. The lipid droplet is an important organelle for hepatitis C virus production. Nat. Cell Biol. **9**:1089–1097.
46. **Moorman, J. P., D. Prayther, D. McVay, Y. S. Hahn, and C. S. Hahn.** 2003. The C-terminal region of hepatitis C core protein is required for Fas-ligand independent apoptosis in Jurkat cells by facilitating Fas oligomerization. Virology **312**:320–329.
47. **Murray, C. L., C. T. Jones, J. Tassello, and C. M. Rice.** 2007. Alanine scanning of the hepatitis C virus core protein reveals numerous residues essential for production of infectious virus. J. Virol. **81**:10220–10231.
48. **Nomura-Takigawa, Y., M. Nagano-Fujii, L. Deng, S. Kitazawa, S. Ishido, K. Sada, and H. Hotta.** 2006. Non-structural protein 4A of hepatitis C virus accumulates on mitochondria and renders the cells prone to undergoing mitochondria-mediated apoptosis. J. Gen. Virol. **87**:1935–1945.
49. **Otsuka, M., N. Kato, H. Taniguchi, H. Yoshida, T. Goto, Y. Shiratori, and M. Omata.** 2002. Hepatitis C virus core protein inhibits apoptosis via enhanced Bcl-xL expression. Virology **296**:84–93.
50. **Petros, A. M., E. T. Olejniczak, and S. W. Fesik.** 2004. Structural biology of the Bcl-2 family of proteins. Biochim. Biophys. Acta **1644**:83–94.
51. **Polster, B. M., J. Pevsner, and J. M. Hardwick.** 2004. Viral Bcl-2 homologs and their role in virus replication and associated diseases. Biochim. Biophys. Acta **1644**:211–227.
52. **Ray, R. B., and R. Ray.** 2001. Hepatitis C virus core protein: intriguing properties and functional relevance. FEMS Microbiol. Lett. **202**:149–156.
53. **Realdon, S., M. Gerotto, F. Dal Pero, O. Marin, A. Granato, G. Basso, M. Muraca, and A. Alberti.** 2004. Proapoptotic effect of hepatitis C virus CORE protein in transiently transfected cells is enhanced by nuclear localization and is dependent on PKR activation. J. Hepatol. **40**:77–85.
54. **Ruggieri, A., T. Harada, Y. Matsuura, and T. Miyamura.** 1997. Sensitization to Fas-mediated apoptosis by hepatitis C virus core protein. Virology **229**:68–76.
55. **Sabile, A., G. Perlemuter, F. Bono, K. Kohara, F. Demaugre, M. Kohara, Y. Matsuura, T. Miyamura, C. Brechot, and G. Barba.** 1999. Hepatitis C virus core protein binds to apolipoprotein AII and its secretion is modulated by fibrates. Hepatology **30**:1064–1076.
56. **Sacco, R., T. Tsutsumi, R. Suzuki, M. Otsuka, H. Aizaki, S. Sakamoto, M. Matsuda, N. Seki, Y. Matsuura, T. Miyamura, and T. Suzuki.** 2003. Anti-apoptotic regulation by hepatitis C virus core protein through up-regulation of inhibitor of caspase-activated DNase. Virology **317**:24–35.
57. **Saito, K., K. Meyer, R. Warner, A. Basu, R. B. Ray, and R. Ray.** 2006. Hepatitis C virus core protein inhibits tumor necrosis factor alpha-mediated apoptosis by a protective effect involving cellular FLICE inhibitory protein. J. Virol. **80**:4372–4379.
58. **Shibue, T., and T. Taniguchi.** 2006. BH3-only proteins: integrated control point of apoptosis. Int. J. Cancer. **119**:2036–2043.
59. **Soo, H. M., A. Garzino-Demo, W. Hong, Y. H. Tan, Y. J. Tan, P. Y. Goh, S. G. Lim, and S. P. Lim.** 2002. Expression of a full-length hepatitis C virus cDNA up-regulates the expression of CC chemokines MCP-1 and RANTES. Virology **303**:253–277.
60. **Takamatsu, M., T. Fujita, and H. Hotta.** 2001. Suppression of serum starvation-induced apoptosis by hepatitis C virus core protein. Kobe J. Med. Sci. **47**:97–112.
61. **Tan, K. O., K. M. Tan, S. L. Chan, K. S. Yee, M. Bevort, K. C. Ang, and V. C. Yu.** 2001. MAP-1, a novel proapoptotic protein containing a BH3-like motif that associates with Bax through its Bcl-2 homology domains. J. Biol. Chem. **276**:2802–2807.
62. **Tan, K. O., K. M. Tan, and V. C. Yu.** 1999. A novel BH3-like domain in BID is required for intramolecular interaction and autoinhibition of pro-apoptotic activity. J. Biol. Chem. **274**:23687–23690.
63. **Tan, Y. J., B. C. Fielding, P. Y. Goh, S. Shen, T. H. Tan, S. G. Lim, and W. Hong.** 2004. Overexpression of 7a, a protein specifically encoded by the severe acute respiratory syndrome coronavirus, induces apoptosis via a caspase-dependent pathway. J. Virol. **78**:14043–14047.
64. **Tan, Y. J., E. Teng, S. Shen, T. H. Tan, P. Y. Goh, B. C. Fielding, E. E. Ooi, H. C. Tan, S. G. Lim, and W. Hong.** 2004. A novel severe acute respiratory syndrome coronavirus protein, U274, is transported to the cell surface and undergoes endocytosis. J. Virol. **78**:6723–6734.
65. **Targett-Adams, P., G. Hope, S. Boulant, and J. McLauchlan.** 2008. Maturation of hepatitis C virus core protein by signal peptide peptidase is required for virus production. J. Biol. Chem. **283**:16850–16859.
66. **Uhlmann, E. J., T. Subramanian, C. A. Vater, R. Lutz, and G. Chinnadurai.** 1998. A potent cell death activity associated with transient high level expression of BCL-2. J. Biol. Chem. **273**:17926–17932.

67. **van Delft, M. F., and D. C. Huang.** 2006. How the Bcl-2 family of proteins interact to regulate apoptosis. Cell Res. **16:**203–213.
68. **Wakita, T., T. Pietschmann, T. Kato, T. Date, M. Miyamoto, Z. Zhao, K. Murthy, A. Habermann, H. G. Krausslich, M. Mizokami, R. Bartenschlager, and T. J. Liang.** 2005. Production of infectious hepatitis C virus in tissue culture from a cloned viral genome. Nat. Med. **11:**791–796.
69. **Walensky, L. D.** 2006. BCL-2 in the crosshairs: tipping the balance of life and death. Cell Death Differ. **13:**1339–1350.
70. **White, E.** 2006. Mechanisms of apoptosis regulation by viral oncogenes in infection and tumorigenesis. Cell Death Differ. **13:**1371–1377.
71. **Willis, S. N., and J. M. Adams.** 2005. Life in the balance: how BH3-only proteins induce apoptosis. Curr. Opin. Cell Biol. **17:**617–625.
72. **Yamanaka, T., M. Uchida, and T. Doi.** 2002. Innate form of HCV core protein plays an important role in the localization and the function of HCV core protein. Biochem. Biophys. Res. Commun. **294:**521–527.
73. **Yao, K., and V. N. Vakharia.** 2001. Induction of apoptosis in vitro by the 17-kDa nonstructural protein of infectious bursal disease virus: possible role in viral pathogenesis. Virology **285:**50–58.
74. **Yasui, K., T. Wakita, K. Tsukiyama-Kohara, S. I. Funahashi, M. Ichikawa, T. Kajita, D. Moradpour, J. R. Wands, and M. Kohara.** 1998. The native form and maturation process of hepatitis C virus core protein. J. Virol. **72:**6048–6055.
75. **Youle, R. J., and A. Strasser.** 2008. The BCL-2 protein family: opposing activities that mediate cell death. Nat. Rev. Mol. Cell Biol. **9:**47–59.
76. **Zhu, N., C. F. Ware, and M. M. Lai.** 2001. Hepatitis C virus core protein enhances FADD-mediated apoptosis and suppresses TRADD signaling of tumor necrosis factor receptor. Virology **283:**178–187.

Virus Research 146 (2009) 41–50

Contents lists available at ScienceDirect

Virus Research

journal homepage: www.elsevier.com/locate/virusres

Efficient replication systems for hepatitis C virus using a new human hepatoma cell line

Nobuyuki Kato[a,*], Kyoko Mori[a], Ken-ichi Abe[a], Hiromichi Dansako[a], Misao Kuroki[a], Yasuo Ariumi[a], Takaji Wakita[b], Masanori Ikeda[a]

[a] Department of Tumor Virology, Okayama University Graduate School of Medicine, Dentistry, and Pharmaceutical Sciences, 2-5-1 Shikata-cho, Okayama 700-8558, Japan
[b] Department of Virology II, National Institute of Infectious Diseases, 1-23-1 Toyama, Shinjuku-ku, Tokyo 162-8640, Japan

ARTICLE INFO

Article history:
Received 29 May 2009
Received in revised form 12 August 2009
Accepted 21 August 2009
Available online 29 August 2009

Keywords:
Hepatitis C virus (HCV)
HCV RNA replication
Li23 cells
Reporter assay for anti-HCV reagents
Infectious HCV production

ABSTRACT

Persistent hepatitis C virus (HCV) infection causes chronic liver diseases and is a serious global health problem. Cell culture-based persistent HCV RNA replication systems and infectious HCV production systems are widely used in HCV research. However, persistent HCV production systems have been developed only for HuH-7 hepatoma cells. Here we found a new human hepatoma cell line, Li23, that enables persistent HCV production and anti-HCV reagent assay. Li23's cDNA expression profile differed from HuH-7's, although the two cells had similar liver-specific expression profiles. We used HCV RNA with a specific combination of adaptive mutations to develop an HCV replicon system and genome-length HCV RNA replicating systems including a reporter assay system. Finally, Li23-derived cells persistently produced infectious virus of an HCV strain. Li23-derived cells are potentially useful for understanding the HCV life cycle and for finding antiviral targets.

1. Introduction

Hepatitis C virus (HCV) infection frequently causes active liver diseases such as chronic hepatitis, cirrhosis, and hepatocellular carcinoma (Choo et al., 1989; Saito et al., 1990; Thomas, 2000). Although the combination of pegylated-interferon (PEG-IFN) and ribavirin is the standard therapy worldwide, only half of the patients receiving this treatment exhibit a sustained virological response (Chevaliez and Pawlotsky, 2007; Hadziyannis et al., 2004). Since more than 170 million people are infected with HCV worldwide, the virus remains a serious global health problem (Thomas, 2000). HCV is an enveloped positive single-stranded RNA virus of the *Flaviviridae* family. The HCV RNA genome encodes a large polyprotein precursor of approximately 3000 amino acids, which is cleaved into 10 proteins in the following order: core, envelope 1 (E1), E2, p7, non-structural 2 (NS2), NS3, NS4A, NS4B, NS5A, and NS5B (Hijikata et al., 1991, 1993; Kato et al., 1990). Although many issues have been addressed since HCV was first identified, the lack of a virus culture system has long been a serious handicap in the fight against HCV infection (Kato and Shimotohno, 2000). The development of an HCV replicon system enabling HCV subgenomic RNA replication in HuH-7 human hepatoma cells has allowed the study of the mechanisms underlying HCV replication (Lohmann et al., 1999). After the first replicon of genotype 1b was developed, HCV replicons derived from several HCV strains appeared, and tissue, genotype, and host ranges were expanded (Ali et al., 2004; Date et al., 2004; Ikeda et al., 2002; Kato et al., 2003a,b; Kishine et al., 2002; Zhu et al., 2003). However, most of RNA replication systems using the culture cells other than HuH-7 cells have been fairly low-level. Furthermore, genome-length HCV RNA replication systems and drug assay systems have been developed (Blight et al., 2002; Ikeda et al., 2002, 2005; Mori et al., 2008; Pietschmann et al., 2002). To date, however, robust genome-length HCV RNA replication and anti-HCV reagent assays have been developed for only one human cell line, HuH-7 (Bartenschlager and Sparacio, 2007; Lindenbach and Rice, 2005). In 2005, an efficient virus production system using the JFH1 genotype 2a strain was developed using HuH-7-derived cell lines (Lindenbach et al., 2005; Wakita et al., 2005; Zhong et al., 2005). In this system also, HuH-7 is still the only cell line that enables persistent HCV production without additional host factors such as CD81 (Gottwein and Bukh, 2008), although transient virus production in human hepatoma cell line LH86 was recently reported (Zhu et al., 2007). Furthermore, it is uncertain whether or not the recent advances obtained from the HuH-7 cell system reflect the general features of the HCV life cycle. Here, we found a new human hepatoma cell line, Li23, that enables robust genome-length

Abbreviations: HCV, hepatitis C virus; PEG-IFN, pegylated-interferon; E1, envelope 1; NS2, non-structural 2; RT-PCR, reverse transcription-polymerase chain reaction; PBS, phosphate-buffered saline; p.i., post-infection; dsRNA, double-stranded RNA; EC_{50}, 50% effective concentration.

* Corresponding author. Tel.: +81 86 235 7385; fax: +81 86 235 7392.
E-mail address: nkato@md.okayama-u.ac.jp (N. Kato).

0168-1702/$ – see front matter © 2009 Elsevier B.V. All rights reserved.
doi:10.1016/j.virusres.2009.08.006

HCV RNA replication. Using Li23-derived cell lines, we developed a novel drug assay system and a persistent HCV production system.

2. Materials and methods

2.1. Cell line

The Li23 cell line, established in 1987, consists of human hepatoma cells from a Japanese male (age 56) and was kindly provided by Drs. Y. Ishikawa and S. Hirohashi (National Cancer Center Research Institute, Tokyo). The Li23 cell line is free of both the hepatitis B virus antigen and HCV (Kato et al., 1995).

2.2. Cell culture

The six HuH-7-derived cell lines: sO cells, harboring the subgenomic replicon RNA of HCV-O (genotype 1b) (Kato et al., 2003a); O cells, harboring a replicative genome-length HCV-O RNA (Ikeda et al., 2005); Oc cured cells, which were created by eliminating HCV RNA from O cells by IFN treatment (Ikeda et al., 2005); OAc cured cells, which were created by eliminating HCV RNA from genome-length HCV-O RNA replicating OA cells (Abe et al., 2007); OR6 cells, harboring the genome-length HCV-O RNA with luciferase as a reporter (Ikeda et al., 2005); RSc cured cells that cell culture-generated HCV-JFH1 (HCVcc) (JFH1 strain of genotype 2a) (Wakita et al., 2005) could infect and efficiently replicate (Ariumi et al., 2007, 2008; Kuroki et al., 2009), or their parental HuH-7 cells were cultured in Dulbecco's modified eagle's medium (DMEM) supplemented with 10% fetal bovine serum (FBS). The sO, O, and OR6 cells were maintained in the presence of G418 (0.3 mg/ml, Geneticin; Invitrogen). Li23 cells were maintained in modified culture medium for the PH5CH8 human immortalized hepatocyte cell line (Ikeda et al., 1998). The medium for Li23 cells consists of F12 medium and DMEM (1:1 in volume) supplemented with 1% FBS, epidermal growth factor (50 ng/ml), insulin (10 μg/ml), hydrocortison (0.36 μg/ml), transferrin (5 μg/ml), linoleic acid (5 μg/ml), selenium (20 ng/ml), prolactin (10 ng/ml), gentamycin (10 μg/ml), kanamycin monosulfate (0.2 mg/ml), and fungizone (0.5 μg/ml). Li23-derived cells harboring the HCV replicon or genome-length HCV RNA were cultured in the above medium supplemented with G418 (0.3 mg/ml). The cured Li23-derived cells were maintained in the above medium without G418. The HeLa and HEK293 cells were cultured in DMEM supplemented with 10% FBS.

2.3. Plasmid construction

To introduce the mutations into plasmid pON/3-5B, pON/C-5B, or pORN/C-5B (Ikeda et al., 2005) (GenBank accession no. AB191333; Supplemental Fig. S1), a PCR-based site-directed mutagenesis method was used as previously described (Abe et al., 2007; Mori et al., 2008).

2.4. RNA synthesis

Plasmid DNAs were linearized with XbaI and used for RNA synthesis with the T7 MEGAscript kit (Ambion) as previously described (Kato et al., 2003a). Synthesized RNA was purified by lithium chloride precipitation and dissolved in nuclease-free water.

2.5. RNA transfection and selection of G418-resistant cells

RNA was transfected to Li23 or Li23-derived cells as previously described (Lohmann et al., 1999). Cells were selected in complete medium with G418 (0.3 mg/ml) and sodium bicarbonate solution (0.15%) for 3 weeks as previously described (Kato et al., 2003a). For the staining of G418-resistant colonies, Coomassie brilliant blue (0.06% in 50% methanol–10% acetic acid) was used as previously described (Ikeda et al., 2005).

2.6. Western blot analysis

The preparation of cell lysates, sodium dodecyl sulfate-polyacrylamide gel electrophoresis and immunoblotting analysis with a PVDV membrane were performed as previously described (Kato et al., 2003a). The antibodies used for the O strain in this study were those against core (CP11; Institute of Immunology), E1 and E2 (a generous gift from Dr. M. Kohara, Tokyo Metropolitan Institute of Medical Science), NS3 (Novocastra Laboratories), NS4A and NS5A (a generous gift from Dr. A. Takamizawa, Research Foundation for Microbial Diseases, Osaka University), and NS5B (a generous gift from Dr. M. Kohara, Tokyo Metropolitan Institute of Medical Science). The antibodies used for the JFH1 strain were those against core (CP11; Institute of Immunology) and NS5B (Murakami et al., 2008). β-Actin antibody (Sigma) was used as the control for the amount of protein loaded per lane. Immunocomplexes were detected by the Renaissance enhanced chemiluminescence assay (PerkinElmer Life Sciences).

2.7. Northern blot analysis

Total RNA from the cultured cells was prepared using an RNeasy extraction kit (Qiagen). Three micrograms of total RNA was used for the analysis. HCV-specific RNA and β-actin mRNA were detected according to a method described previously (Ikeda et al., 2005; Kato et al., 2003a). The synthetic RNA transcribed from pON/3-5B, pON/C-5B, or pORN/C-5B (10^7 and 10^8 genome equivalents spiked into cellular total RNA) was used to compare HCV RNA levels.

2.8. Quantification of HCV RNA

Quantitative reverse transcription-polymerase chain reaction (RT-PCR) analysis for HCV RNA was performed using a real-time LightCycler PCR as described previously (Ikeda et al., 2005). We used the following forward and reverse primer sets for the real-time LightCycler PCR: HCV-O, 5′-AGAGCCATAGTGGTCTGCGG-3′ (forward), 5′-CTTTCGCGACCCAACACTAC-3′ (reverse); and HCV-JFH1, 5′-AGAGCCATAGTGGTCTGCGG-3′ (forward), 5′-CTTTCGCAACCCAACGCTAC-3′ (reverse). Experiments were done in triplicate.

2.9. Preparation of cured cells

To prepare cured cells, the cells harboring the HCV replicon or genome-length HCV RNA were treated with IFN-γ as described previously (Abe et al., 2007). Briefly, the cells were treated with IFN-γ (1000 IU/ml) in the absence of G418. The treatment was continued for 3 weeks with the addition of IFN-γ at 4-day intervals. The cured cells obtained from O, OA, sOL, OL8, OL11, OL14, ORL8, and ORL11 cells were named Oc, OAc, sOLc, OL8c, OL11c, OL14c, ORL8c, and ORL11c, respectively. RT-PCR confirmed the absence of HCV RNA in these cured cells.

2.10. Immunofluorescence and confocal microscopic analyses

Four days after the cells were seeded on the collagen-coated coverslip, they were fixed with 3% paraformaldehyde in phosphate-buffered saline (PBS) and then permeabilized in 0.1% Triton X-100 in PBS at room temperature. After blocking with 1% bovine serum albumin, the cells were incubated with the primary antibodies and then with the secondary antibody. The primary antibodies used to detect the core and dsRNA were anti-core (CP11; Institute of Immunology) and anti-double-stranded (ds) RNA (K1; English and

Scientific Consulting), respectively. The primary antibodies used to detect NS5B of O strain and JFH1 strain were anti-NS5B (a generous gift from Dr. M. Kohara, Tokyo Metropolitan Institute of Medical Science) and anti-NS5B (Murakami et al., 2008), respectively. The secondary antibody was Cy2-conjugated anti-mouse secondary antibody or FITC-conjugated anti-rabbit secondary antibody (for NS5B of JFH1) (Jackson ImmunoResearch). The nuclei were stained with 4′,6-diamidino-2-phenylindole (Sigma). The coverslips were mounted on glass slides by PermaFluor Aqueous Mountant (ThermoFisher) and then the cells were photographed under a confocal laser scanning microscope (LSM510; Carl Zeiss).

2.11. cDNA microarray analysis

HuH-7, Oc, OAc, Li23, OL8, OL11, OL8c, and OL11c cells (1×10^6 each) were plated onto 10-cm diameter dishes and cultured for 2 days in the absence of G418. Total RNAs from these cells were prepared using the RNeasy extraction kit (Qiagen). cDNA microarray analysis was performed by Dragon Genomics Center of Takara Bio. (Otsu, Japan) through an authorized Affymetrix service provider. cDNA was synthesized by the GeneChip T7-Oligo(dT) Promoter Primer Kit (Affymetrix) and TaKaRa cDNA Synthesis Kit (Takara Bio) from 3 μg total RNA. Biotinylated complementary RNA (cRNA) was synthesized by the IVT Labeling Kit (Affymetrix). Following fragmentation, 10 μg of cRNA was hybridized for 16 h at 45 °C on the GeneChip Human Genome U133 Plus 2.0 Array. GeneChips were washed and stained in the Affymetrix Fluidics Station 450, and then were scanned using GeneChip Scanner 3000 7G. Single array analysis was calculated by Microarray Suite version 5.0 (MAS5.0) with the Affymetrix setting. Differentially expressed genes were selected by comparing HuH-7-derived cells and Li23-derived cells.

2.12. RT-PCR

RT-PCR was performed to detect cellular mRNA as described previously (Dansako et al., 2003). Briefly, total RNA (2 μg) was reverse-transcribed with M-MLV reverse transcriptase (Invitrogen) using an oligo dT primer (Invitrogen) according to the manufacturer's protocol. One-tenth of synthesized cDNA was used for PCR. The primers and PCR cycles used in this study are listed in Supplemental Table 1.

2.13. Quantification of HCV core protein

The levels of the core protein in the culture supernatants were determined by enzyme-linked immunosorbent assay (Mitsubishi Kagaku Bio-Clinical Laboratories).

2.14. Renilla luciferase assay for anti-HCV reagents

To monitor the effects of anti-HCV reagents, the cells were plated onto 24-well plates (2×10^4 cells per well) and cultured with the medium for Li23-derived cells in the absence of fungizone and G418 for 24 h. The cells were then treated with anti-HCV reagent at several concentrations for 72 h (sometimes 24 or 48 h), or the cells were treated with a combination of IFN-α and another anti-HCV reagent at several concentrations for 72 h. After treatment, the cells were subjected to luciferase assay using the renilla luciferase assay system according to the manufacturer's protocol (Promega). A manual Lumat LB 9501/16 luminometer (EG&G Berthold) was used to detect luciferase activity. The experiments were performed in at least triplicate.

2.15. Cell viability

To examine the cytotoxic effects of anti-HCV reagents on the cells, the cells were plated onto 24-well plates (2×10^4 cells per well) and cultured for 24 h. They were then treated with or without anti-HCV reagents for 72 h in the absence of G418. The viable cells were then counted in an improved Neubauer-type hemotocytometer after Trypan blue dye (Invitrogen) treatment. The experiments were performed in triplicate.

2.16. Infection of cells with secreted HCV

The inoculum for HCV infection was the culture medium of RSc cells (Ariumi et al., 2007, 2008; Kuroki et al., 2009) at 145 days after transfection with JFH1 RNA *in vitro* synthesized from pJFH1 (Wakita et al., 2005). This inoculum was passed through a 0.2-μm filter after low-speed centrifugation before use for infection. We seeded cells 24 h before infection at a density of 2×10^4 cells per well in a 24-well plate. We infected cells with 100 μl (equivalent to $10^{4.3}$ $TCID_{50}$) of inoculum for 2 h, washed them, added complete medium and cultured them for a maximum of 30 days with adequate passage of the cells. In some cases, at 7 or 8 days p.i., supernatant was used as an inoculum for the next HCV infection. The cells at 7 or 14 days p.i. were used to detect HCV proteins by Western blot analysis, to quantify HCV RNA by quantitative RT-PCR or to analyze the immunofluorescence of HCV proteins or dsRNA.

3. Results

3.1. Efficient replication system with HCV replicon or genome-length HCV RNA using human hepatoma Li23 cells

We previously established several genome-length HCV RNA (O strain of genotype 1b) replicating cell lines and found that a specific combination of adaptive mutations – either Q1112R, P1115L, and S2200R (QR,PL,SR) or Q1112R, K1609E, and S2200R (QR,KE,SR) – drastically enhanced the level of genome-length HCV RNA replication (Abe et al., 2007; Ikeda et al., 2005). This finding led us to hypothesize that such combinations of adaptive mutations may overcome the barrier that has made HuH-7 the only cell line thus far to allow the robust replication of genome-length HCV RNA. To test this hypothesis, HCV replicon RNA (ON/3-5B) possessing QR,PL,SR or QR,KE,SR (Supplemental Fig. 1) was transfected into various kinds of human cell lines (HuH-6, Li21, Li23, Li24, PH5CH, OUMS29, IHH10.3, IHH12 etc.), and the G418 selection was performed as described previously (Kato et al., 2003a). Although we failed to obtain the G418-resistant colonies in the most cell lines, fortunately, we found that the Li23 human hepatoma cell line gave only G418-resistant colonies (Fig. 1A). Approximately 200 and 700 colonies obtained from ON/3-5B/QR,PL,SR and ON/3-5B/QR,KE,SR-transfected cells, respectively, were pooled. Western blot analysis revealed that the expression levels of HCV proteins NS5A and NS5B were much higher in ON/3-5B/QR,KE,SR-derived colonies than in ON/3-5B/QR,PL,SR-derived colonies (Fig. 1B). We used the former for further analysis and referred to them as sOL cells. We demonstrated that the replicon in sOL cells showed a high level of sensitivity to anti-HCV reagents, similar to the level shown by the replicon (ON/3-5B/SR) in sO cells (Kato et al., 2003a) (Fig. 1C).

To obtain a source of cells with which to develop a genome-length HCV RNA replication system, we prepared cured cells (sOLc) from sOL cells by IFN-γ treatment, because cured cells are known to extremely enhance HCV RNA replication levels (Ikeda et al., 2005; Kato et al., 2003a). A genome-length HCV RNA (ON/C-5B/QR,KE,SR; Supplemental Fig. 1) was transfected into sOLc cells. Following G418 selection, many colonies were obtained (Fig. 2A). Fourteen

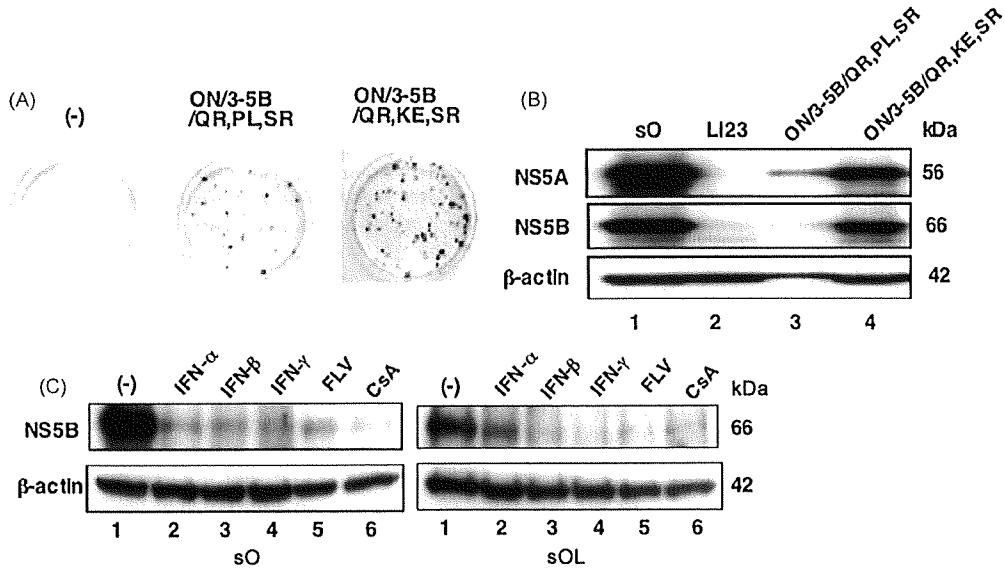

Fig. 1. Li23-derived cells harboring HCV replicon. (A) G418-resistant colonies from Li23 cells transfected with replicon RNA. ON/3-5B RNA with three additional mutations (ON/3-5B/QR,PL,SR or ON/3-5B/QR,KE,SR) was transfected into Li23 cells. The panels show G418-resistant colonies (57 colonies/μg RNA for ON/3-5B/QR,PL,SR and 132 colonies/μg RNA for ON/3-5B/QR,KE,SR) that were stained with Coomassie brilliant blue at 3 weeks after RNA transfection. (B) Western blot analysis of Li23-derived G418-resistant cells for HCV proteins NS5A and NS5B. Lane 1, sO (HuH-7-derived cell line harboring HCV replicon, ON/3-5B/SR); lane 2, Li23 as a negative control; lane 3, polyclonal G418-resistant cells obtained by transfection with ON/3-5B/QR,PL,SR RNA; lane 4, polyclonal G418-resistant cells (sOL) by transfection with ON/3-5B/QR,KE,SR RNA. (C) Sensitivity of sOL replicon to anti-HCV reagents. sOL cells were treated with IFN-α (lane 2, 20 IU/ml), IFN-β (lane 3, 20 IU/ml), IFN-γ (lane 4, 20 IU/ml), fluvastatin (FLV) (lane 5, 5 μM), or cyclosporine A (CsA) (lane 6, 0.5 μg/ml) for 5 days. Lane 1 shows no treatment. For comparison, sO cells were treated as well as sOL cells. NS5B was detected by Western blot analysis.

colonies (referred to as OL1–OL14) and a mixture of approximately 200 other colonies (referred to as OL) were successfully proliferated as cell lines. Using quantitative RT-PCR, we selected OL8, OL11, and OL14 because of their high levels (>9 × 10^6 copies/μg total RNA) of HCV RNA, although the titer of HCV RNA from genome-length HCV RNA replicating HuH-7-derived O cells (Ikeda et al., 2005) was approximately 4.5 × 10^7 copies/μg total RNA (Supplemental Fig. 2). We also demonstrated that the HCV sequence was not

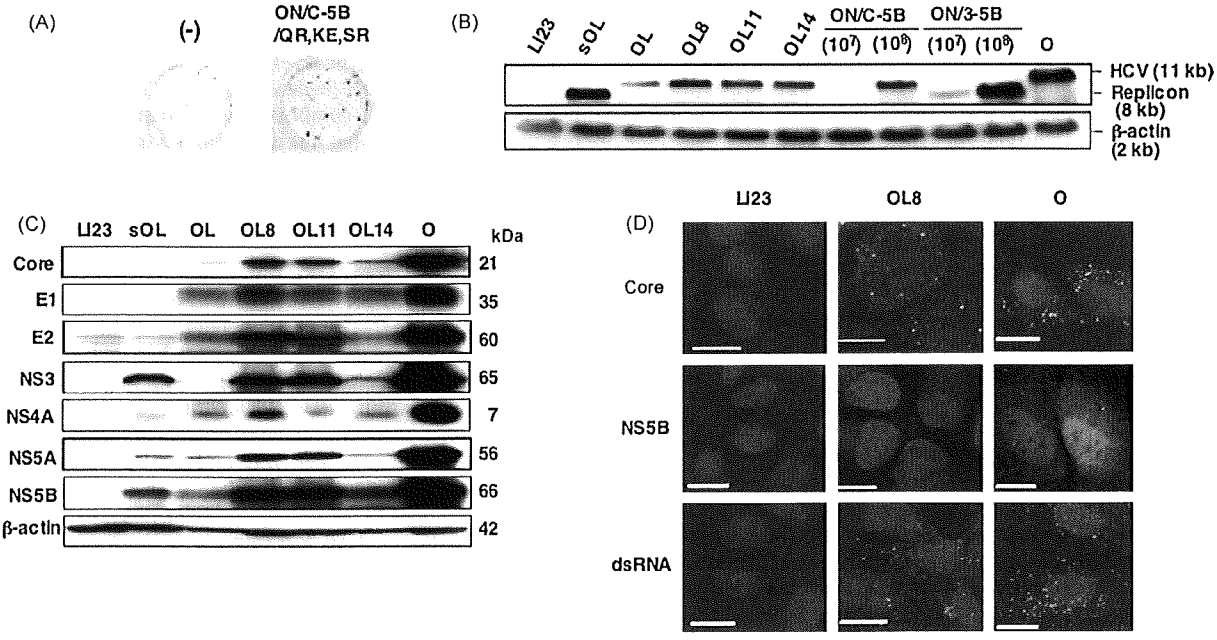

Fig. 2. Establishment of Li23-derived cell lines harboring replicative genome-length HCV RNA. (A) G418-resistant colonies from sOLc cells transfected with genome-length HCV RNA (ON/C-5B/QR,KE,SR). The panels show G418-resistant colonies (100 colonies/μg RNA) that were stained with Coomassie brilliant blue at 3 weeks after RNA transfection. (B) Northern blot analysis of total RNA prepared from sOL cells and genome-length HCV RNA-replicating cells (OL, OL8, OL11, and OL14). Synthetic RNA, given number of ON/C-5B or ON/3-5B RNA. HuH-7-derived O cells harboring replicative genome-length HCV RNA (ON/C-5B/KE,SR) and Li23 cells served as positive and negative controls, respectively. (C) Western blot analysis of sOL and genome-length HCV RNA-replicating cells (OL, OL8, OL11, and OL14) for HCV proteins, core, E1, E2, NS3, NS4A, NS5A, and NS5B. O cells and Li23 cells served as positive and negative controls, respectively. (D) Immunofluorescence analysis of OL8 cells. The cells were processed and stained with anti-core, anti-NS5B, or anti-dsRNA antibodies and Cy2-conjugated secondary antibody. The O cells and Li23 cells served as positive and negative controls, respectively. Bar, 20 μm.

integrated into the genomic DNA in OL, OL8, OL11, OL14, or sOL cells (data not shown). Northern and Western blot analyses also showed that the levels of HCV RNA and proteins in OL8 and OL11 cells were somewhat lower than those in O cells (Fig. 2B and C). Immunofluorescence analysis of the intracellular localization of HCV proteins and dsRNA, which is an intermediate of RNA replication, showed that the staining levels of HCV proteins and dsRNA located in the cytoplasm of OL8 cells, were also comparable to those in O cells (Fig. 2D). Both OL8 and O cells had two types of core protein staining patterns (detergent-resistant dots or patches and detergent-sensitive ring-like structures), as described previously (Matto et al., 2004) in HuH-7 cells harboring the genome-length HCV RNA (Con1 strain of genotype 1b) (Fig. 2D). These results suggest that robust replication of genome-length HCV RNA occurs in OL8 and OL11 cells. We performed sequence analysis of HCV RNAs derived from OL8, OL11, and OL14 cells, but no additional mutations were detected commonly among the three independent clones sequenced (data not shown). This suggested that no mutations other than Q1112R, K1609E, and S2200R are needed for genome-length HCV RNA replication in Li23-derived cells.

3.2. Genes differentially expressed between Li23- and HuH-7-derived cells

RT-PCR analysis revealed that Li23 and HuH-7 cells had similar liver-specific gene expression profiles (Fig. 3A). However, there is no information regarding the Li23-specific gene expression profile. To address this, we performed cDNA microarray analysis using total RNAs prepared from Li23, OL8, OL11, cured OL8 (OL8c), and OL11c cells in addition to HuH-7, Oc (Ikeda et al., 2005), and OAc (Abe et al., 2007). As the first step in this analysis, we selected 206 and 326 genes whose expression levels were upregulated and downregulated at ratios of more than 2^5 and less than 2^{-5} in Li23 vs. HuH-7, respectively. Then, from among those selected in the first step, we performed an additional selection of genes whose expression levels were commonly upregulated or downregulated among Li23-derived cells when compared with HuH-7-derived cells, and each of several already-known genes were identified (data not shown). Fig. 3B shows the results of RT-PCR regarding the representative genes belonging to such a category in the expression levels between Li23- and HuH-7-derived cells. The most characteristic feature of Li23-derived cells was the high expression levels of cancer antigens (NY-ESO-1, MAGEA, etc.) compared with no expression in HuH-7-derived cells (Fig. 3B). We demonstrated that such drastic differences were not attributable to differences in culture media (Supplemental Fig. 3). These results exclude the possibility that OL8 and OL11 cells are derived from contamination of HuH-7-derived cells. On the other hand, this microarray analysis revealed that HuH-7- and Li23-derived cells showed similar expression levels of CD81, scavenger receptor class B type I (SR-BI), Claudin-1, and Occludin, which have been identified as the host factors for HCV entry (Burlone and Budkowska, 2009). RT-PCR analysis confirmed them (Fig. 3C).

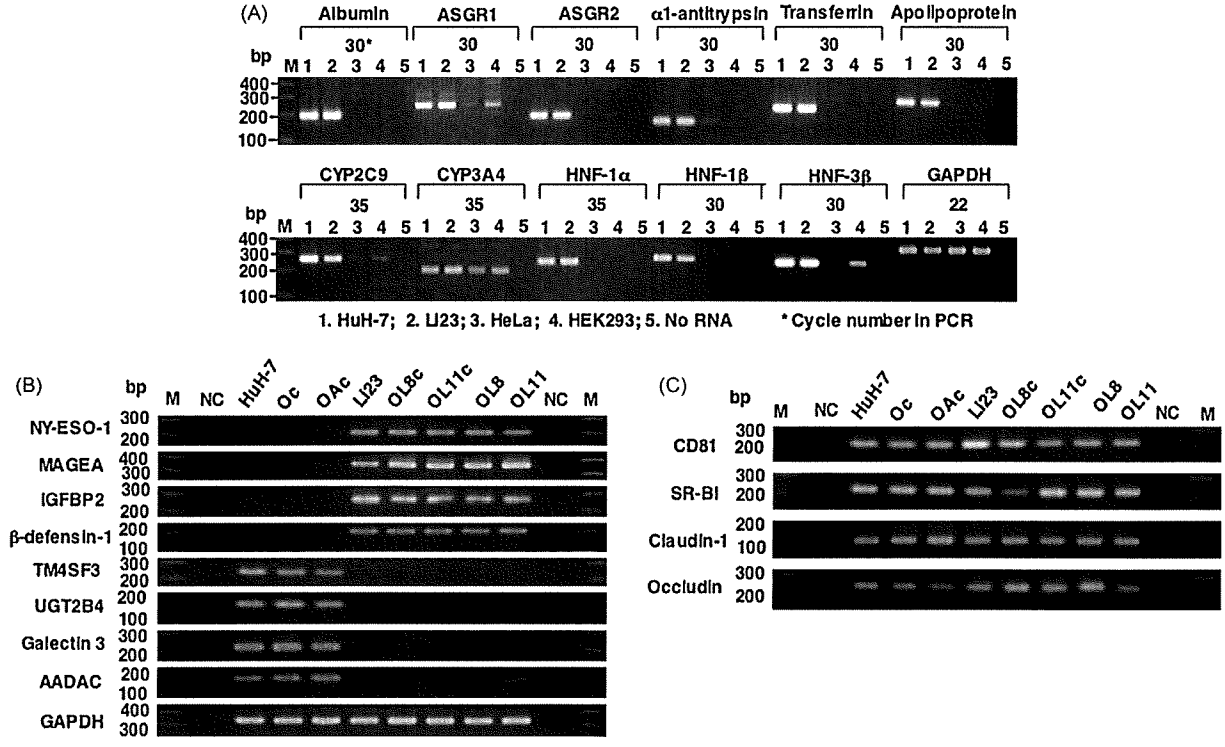

Fig. 3. Representative genes differentially expressed among Li23- and HuH-7-derived cells. (A) Li23 and HuH-7 cells showed similar liver-specific gene expression profiles. Total RNAs prepared from HuH-7, Li23, HeLa, and HEK293 cells were subjected to RT-PCR to detect liver-specific mRNAs using the primer sets listed in Supplementary Table 1. Presented data are the results of the following mRNA species: albumin, asialoglycoprotein receptor 1 (ASGR1), ASGR2, α1-antitrypsin, transferrin, apolipoprotein, cytochrome P450 2C9 (CYP2C9), CYP3A4, hepatocyte nuclear factor 1α (HNF-1α), HNF-1β, and HNF-3β. (B) Representative genes that were differentially expressed between HuH-7-derived cell lines and Li23-derived cell lines. Total RNAs prepared from HuH-7-derived cells (HuH-7, Oc, and OAc) and Li23-derived cells (Li23, OL8c, OL11c, OL8, and OL11) were subjected to RT-PCR using the primer sets listed in Supplementary Table S1. Lane M, 100 bp DNA ladder; NC, no RNA. The data presented are the results of the following mRNA species: cancer testis antigen (NY-ESO-1), melanoma-specific antigen family A (MAGEA), insulin-like growth factor binding protein 2 (IGFBP2), β-defensin-1, transmembrane 4 superfamily member 3 (TM4SF3), UDP glycosyltransferase 2 family polypeptide B4 (UGT2B4), galectin 3, and arylacetamide deacetylase (AADAC). Glyceraldehyde-3-phosphate dehydrogenase (GAPDH) served as an internal control. (C) Expression levels of CD81, SR-BI, Claudin-1, and Occludin between HuH-7- and Li23-derived cells. RNA preparation and RT-PCR were performed as described in (B).

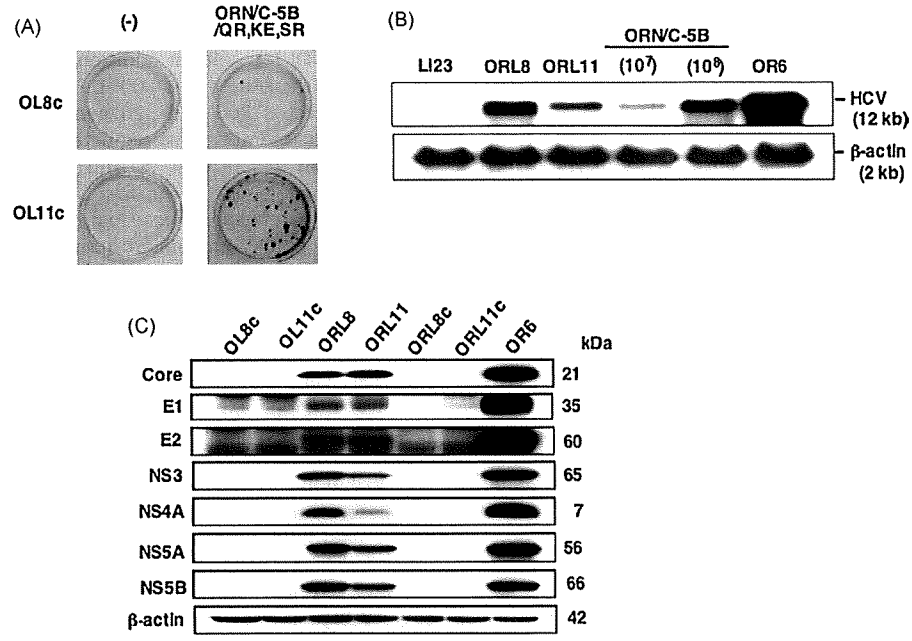

Fig. 4. Establishment of OL8- and OL11-derived cell lines harboring replicative genome-length HCV RNA encoding renilla luciferase. (A) G418-resistant colonies from OL8c or OL11c cells transfected with genome-length HCV RNA (ORN/C-5B/QR,KE,SR) encoding renilla luciferase gene. The panels show G418-resistant colonies that were stained as described in Fig. 1A. (B) Northern blot analysis of total RNA prepared from genome-length HCV RNA replicating ORL8 and ORL11 cells. Synthetic RNA, given number of synthetic ORN/C-5B RNA; Li23, negative control. HuH-7-derived OR6 cells replicating genome-length HCV RNA encoding renilla luciferase gene (ORN/C-5B/KE,SR) served as positive control. (C) Western blot analysis of ORL8 and ORL11 cells for HCV proteins, core, E1, E2, NS3, NS4A, NS5A, and NS5B. OL8c, OL11c, ORL8c, and ORL11c, negative controls; OR6, positive control.

3.3. *Development of new luciferase reporter assay systems that facilitate the quantitative monitoring of HCV RNA replication*

Since the reporter assay system using HuH-7-derived OR6 cells, which robustly replicates genome-length HCV RNA encoding renilla luciferase, is potentially useful for the quantitative evaluation of anti-HCV activity (Ikeda et al., 2005, 2006; Ikeda and Kato, 2007), we have tried to develop an Li23-derived assay system corresponding to the OR6 assay system. A genome-length HCV RNA encoding renilla luciferase (ORN/C-5B/QR,KE,SR) (Supplemental Fig. 1) was transfected into OL8c or OL11c cells. Following G418 selection, several OL8c colonies and several hundred OL11c colonies were obtained from the cells transfected with ORN/C-5B/QR,KE,SR (Fig. 4A). Regarding ORN/C-5B/QR,KE,SR, 9 OL8c-derived clones and 16 OL11c-derived clones were successfully proliferated as cell lines. Each clone possessing the highest

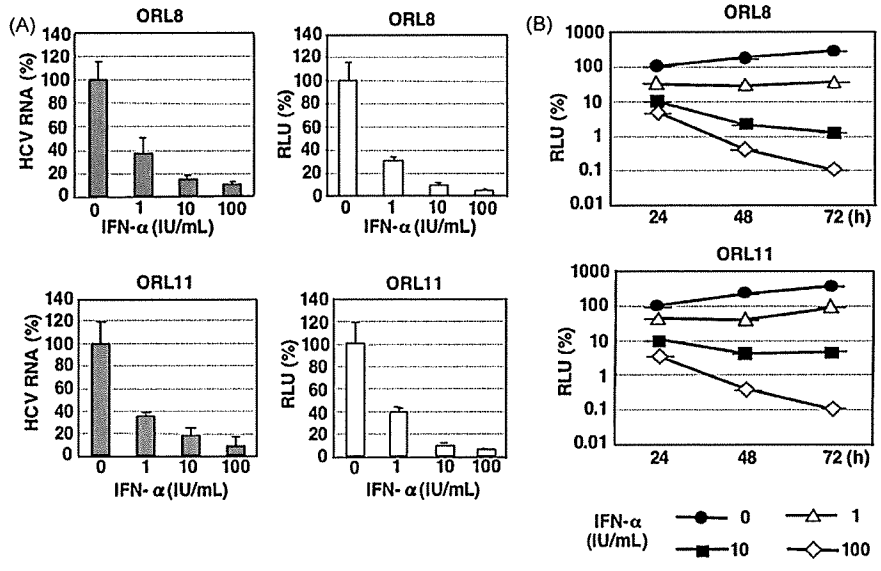

Fig. 5. ORL8 and ORL11 reporter assay system to monitor genome-length HCV RNA replication. (A) Renilla luciferase activity is correlated with HCV RNA level. The ORL8 (upper panels) and ORL11 (lower panels) cells were treated with IFN-α (0, 1, 10, and 100 IU/ml) for 24 h, and then luciferase reporter assay (right panels) and quantitative RT-PCR (left panels) were performed. The relative luciferase activity (RLU) (%) or HCV RNA (%) calculated at each point, when the level of luciferase activity or HCV RNA in non-treated cells was assigned to be 100%, is presented here. (B) IFN-α sensitivity of HCV RNA replication in ORL8 and ORL11 cells. The ORL8 (upper panel) and ORL11 (lower panel) cells were treated with IFN-α (0, 1, 10, and 100 IU/ml); the luciferase assay was performed at 24, 48, and 72 h after the treatment. The RLU (%) calculated at each point, when the luciferase activity of non-treated cells at 24 h was assigned to be 100%, is presented here. The experiments were performed in at least triplicate.

titer of HCV RNA was selected by quantitative RT-PCR and was thereafter referred to as ORL8 and ORL11 (data not shown). We demonstrated that the HCV RNA sequence was not integrated into the genomic DNA in ORL8 or ORL11 cells (data not shown). Northern and Western blot analyses showed that ORL8 and ORL11 cells expressed sufficient levels of HCV RNA and proteins for the quantitative monitoring of HCV RNA replication, although these levels were somewhat lower than those in OR6 cells (Fig. 4B and C). We performed sequence analysis of HCV RNAs derived from ORL8 and ORL11 cells, but no additional mutations were detected commonly among the three independent clones sequenced (data not shown). We demonstrated good correlations between the levels of luciferase activity and HCV RNA in ORL8 and ORL11 cells (Fig. 5A), as we previously demonstrated in OR6 cells treated with IFN-α for 24 h (Ikeda et al., 2005). Time course assays (24, 48, and 72 h) on IFN-α treatment demonstrated that the luciferase activity decreased in a dose- and time-dependent manner, and revealed that the luciferase activity had decreased to less than 0.1% at 72 h after treatment with 100 IU/ml IFN-α (Fig. 5B).

3.4. ORL8 and ORL11 assay systems are frequently more sensitive than the OR6 assay system

Using ORL8 and ORL11 assay systems, we evaluated the anti-HCV activities of representative reagents identified by HuH-7-derived assay systems (Ikeda and Kato, 2007; Moriishi and Matsuura, 2007). For the sake of comparison, we also evaluated these activities using the OR6 assay system along with the same culture medium that we used for the ORL8 and ORL11 assays, since we had already confirmed that HCV RNA in OR6 cells was efficiently replicated using this culture medium (data not shown). First, we measured the 50% effective concentration (EC_{50}) of IFN-α against HCV RNA replication. The EC_{50} values of IFN-α in ORL8, ORL11, and OR6 assays were assigned as 0.13, 0.30, and 0.40 IU/ml, respectively, without suppression of cell growth (Fig. 6A). Regarding IFN-β, IFN-γ, and cyclosporine A also, the ORL8 and ORL11 assays were each more sensitive than the OR6 assay (Fig. 6B). It is noteworthy that the EC_{50} values of fluvastatin and simvastatin in the ORL8 and ORL11 assays were fairly lower than those in the OR6 assay (Fig. 6B). In contrast, we observed that the OR6 assay for geldanamycin was slightly more sensitive than the ORL8 or ORL11 assay (Fig. 6B). When the number of cells without treatment was compared to that of cells with treatment, no significant decrease in cell number was observed following treatment with anti-HCV reagents used in Fig. 6B (data not shown). Co-treatment of IFN-α and fluvastatin also demonstrated that the ORL8 and ORL11 assays were much more sensitive than the OR6 assay (Fig. 6C), indicating that these two systems are powerful biosensors of RNA viral replication.

3.5. Persistent reproduction of HCV life cycle in Li23-derived cells

A most interesting point is whether or not infectious HCV is produced in Li23-derived cell lines and thus enables robust HCV RNA replication. To clarify this point, we used HCV-JFH1 (genotype 2a), the only infectious HCV molecular clone identified in a cell culture to date (Lindenbach et al., 2005; Wakita et al., 2005; Zhong et al.,

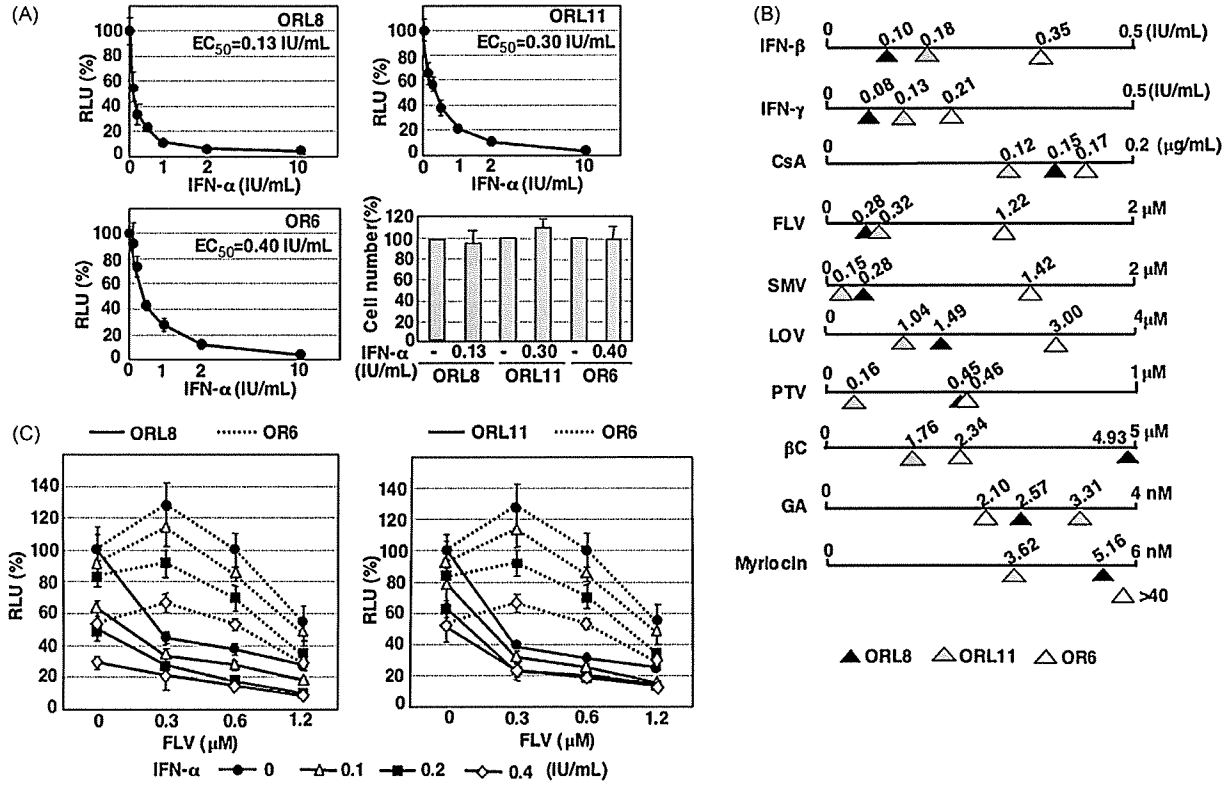

Fig. 6. The diverse effects of anti-HCV reagents in ORL8, ORL11, and OR6 assay systems. (A) IFN-α sensitivities on genome-length HCV RNA replication in ORL8, ORL11, and OR6 assay systems. The ORL8, ORL11, and OR6 cells were treated with IFN-α (0, 0.06, 0.13, 0.25, 0.5, 1, 2, and 10 IU/ml) for 72 h, and then luciferase assay was performed as described in Fig. 5A. ORL8, ORL11, and OR6 cells were cultured in the absence or presence of IFN-α at each 50% effective concentration (EC_{50}) for 72 h, and then the cells were counted as described in Section 2. (B) Diverse EC_{50} values of anti-HCV reagents on genome-length HCV RNA replication in ORL8, ORL11, and OR6 cells. ORL8, ORL11, and OR6 cells were treated with several different concentrations of IFN-β, IFN-γ, CsA, FLV, simvastatin (SMV), lovastatin (LOV), pitavastatin (PTV), β-carotene (βC), geldanamycin (GA), or myriocin for 72 h, after which luciferase assay was performed as described in Fig. 5A. EC_{50} values were calculated from the data of each triplicate assay. (C) ORL8 and ORL11 assay systems are more sensitive than the OR6 assay system in the combination analysis of IFN-α and FLV. ORL8, ORL11, and OR6 cells were treated with a combination of IFN-α (0, 0.1, 0.2, and 0.4 IU/ml) and FLV (0, 0.3, 0.6, and 1.2 μM) for 72 h, after which a luciferase assay was performed as described in Fig. 5A.

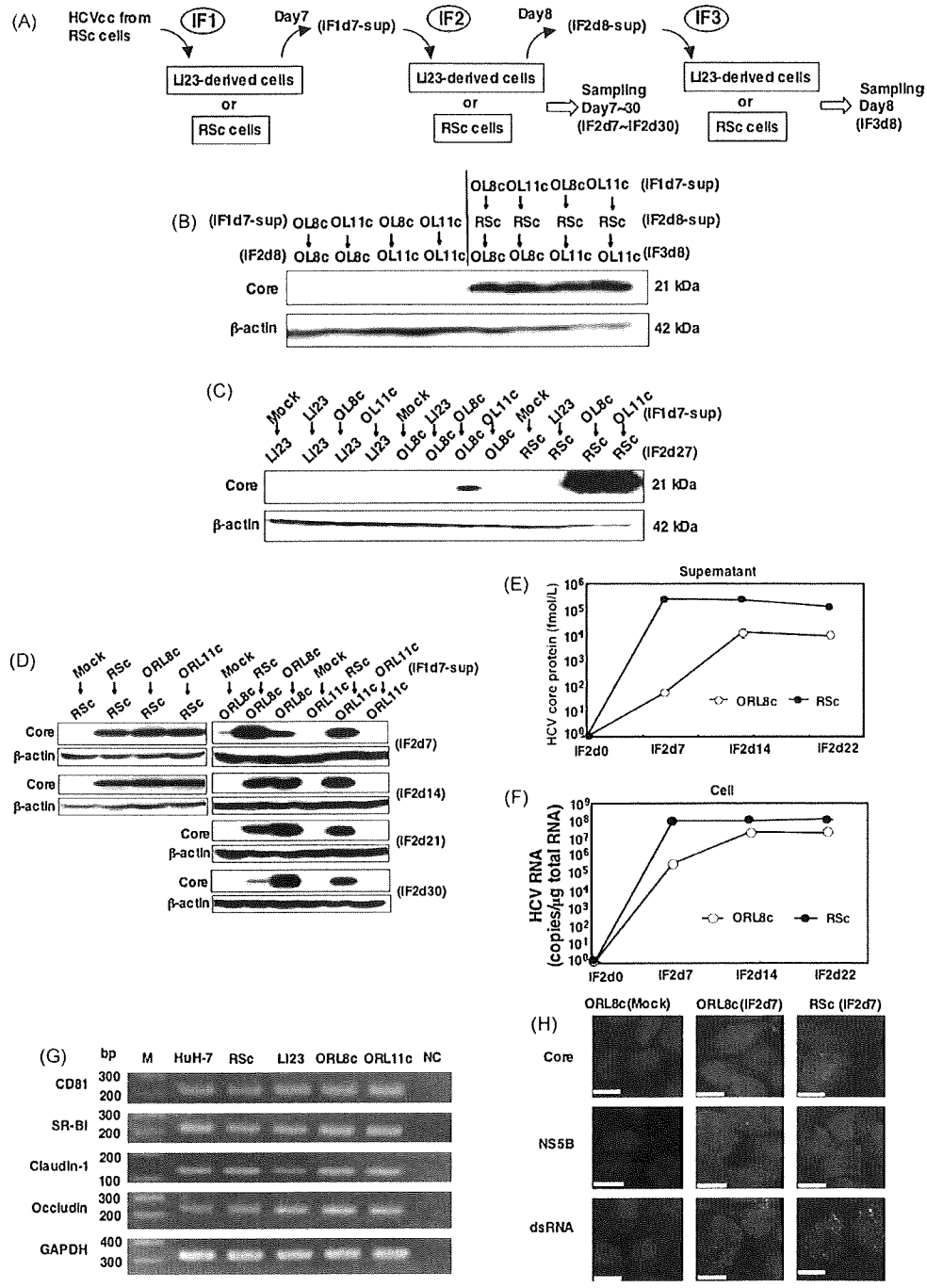

Fig. 7. Reproduction of HCV life cycle in OL8c and ORL8c cells. (A) Flow chart of experiments on HCVcc infection. A time schedule for HCVcc infection and sampling is shown. IF1d7-sup refers to the supernatant of the first-infected cells at 7 days p.i. IF2d7 refers to the secondly infected cells at 7 days p.i. (B) Production of infectious HCV from HCVcc-infected OL8c and OL11c cells. OL8c or OL11c cells were infected with HCVcc produced from RSc cells, and each supernatant at 7 days p.i. (IF1d7-sup) was used for inoculation to OL8c, OL11c, or RSc cells. Western blot analysis was performed to detect HCV core protein in OL8c or OL11c cells at 8 days p.i. (IF2d8). The supernatant (IF2d8-sup) from RSc cells at 8 days p.i. was used for further inoculation to OL8c or OL11c cells. Western blot analysis was performed for the detection of HCV core protein in OL8c or OL11c cells at 8 days p.i. (IF3d8). (C) HCVcc produced from OL8c cells is infectious to OL8c cells. The supernatants (IF1d7-sup) described in (B) were used for inoculation to OL8c and RSc cells. Li23 cells were used as negative controls. Western blot analysis was performed to detect HCV core protein in OL8c, RSc, or Li23 cells at 27 days p.i. (IF2d27). (D) Persistent production of infectious HCVcc from ORL8c cells. ORL8c or ORL11c cells were infected with HCVcc produced from RSc cells, and each supernatant at 7 days p.i. (IF1d7-sup) was used for inoculation to ORL8c or ORL11c cells. RSc cells were used as positive controls. Western blot analysis was performed to detect HCV core protein in ORL8c or ORL11c cells at 7, 14, 21, and 30 days p.i. (IF2). HCV core protein in RSc cells at 7 and 14 days p.i. was also detected by Western blot analysis. (E) Secretion of HCV core protein in culture supernatant. The culture supernatants (IF2d7-, IF2d14-, and IF2d22-sup) of ORL8c or RSc cells were used to determine the levels of core protein by enzyme-linked immunosorbent assay. Experiments were performed in triplicate. (F) Levels of HCV RNA in HCVcc-infected cells. The levels of intracellular HCV RNAs of ORL8c or RSc cells (IF2d7, IF2d14, and IF2d22) were determined by quantitative RT-PCR. Experiments were performed in triplicate. (G) Expression levels of CD81, SR-BI, Claudin-1, and Occludin among RSc, ORL8c, and ORL11c cells. RNA preparation and RT-PCR were performed as described in Fig. 3B. (H) Immunofluorescence analysis of HCVcc-infected cells. ORL8c or RSc cells (IF2d7) were processed and stained with anti-core, anti-NS5B, and anti-dsRNA antibodies and Cy2-conjugated secondary antibody. Mock-infected ORL8c cells served as negative controls. Bar, 20 μm.

2005), and various Li23-derived cell lines obtained in this study (Supplemental Table 2). A flow chart of the expression procedure is shown in Fig. 7A.

Since we detected the transient expression of HCV-JFH1 RNA in OL8c and OL11c cells (Supplemental Fig. 4A), we examined the susceptibility of OL1c, OL2c, OL3c, OL4c, OL8c, OL11c, or OL14c cells to cell culture-generated HCV-JFH1 (HCVcc) produced from HuH-7-derived RSc cells that HCVcc could infect and efficiently replicate (Ariumi et al., 2007, 2008; Kuroki et al., 2009). At 16 days post-infection (p.i.), the core protein was detected in OL2c, OL3c, OL8c, OL11c, and OL14c cells, but not in OL1c and OL4c cells (Supplemental Fig. 4B), indicating that most OLc series cells exhibit good susceptibility to HCVcc. In this context, the supernatant (IF1d7-sup) of HCVcc-infected OL8c or OL11c cells at 7 days p.i. was inoculated to naïve OL8c or OL11c cells; however, we failed to detect the core protein in the cells (IF2d8) at 8 days p.i. (Fig. 7B). However, when the supernatant (IF2d8-sup) of IF1d7-sup-inoculated RSc cells at 8 days p.i. was inoculated to naïve OL8c or OL11c cells, core expression was strongly detected in either case at 8 days p.i. (IF3d8) (Fig. 7B). This suggested that small amount of infectious HCV was produced from OL8c or OL11c cells. Accordingly, the expression of core protein was detected in IF1d7-sup-inoculated OL8c cells, but not in OL11c cells, at 27 days p.i. (IF2d27) (Fig. 7C), indicating that OL8c-derived HCVcc may infect and replicate in naïve OL8c cells. This finding leads to the assumption that ORL8c or ORL11c cells are better than OL8c cells, because ORL8c and ORL11c cells are derived from luciferase reporter full-length HCV RNA-replicating cells (ORL8 and ORL11), and because they each have a more permissible environment for HCV RNA replication. To test this hypothesis, RSc-derived HCVcc was commonly used in order to avoid the issue of uncertain efficiency of RNA transfection to RSc, ORL8c, or ORL11c cells. RSc-derived HCVcc was inoculated to naïve RSc, ORL8c, or ORL11c cells; and RSc, ORL8c, or ORL11c-derived IF1d7-sup was further inoculated to naïve RSc, ORL8c, or ORL11c cells. Expectedly, core expression in the ORL8c cells inoculated with ORL8c-derived IF1d7-sup was strongly detected until at least 30 days p.i. (IF2d30) (Fig. 7D). The level of core protein in the ORL8c cells was equivalent to that in the RSc cells inoculated with RSc, ORL8c, or ORL11c-derived IF1d7-sup (Fig. 7D). Regarding the NS5B expression, similar results were obtained (data not shown). These results suggest that HCV production in ORL8c cells is comparable to that in RSc cells. In contrast, core protein was not detected in ORL11c cells inoculated with ORL11c-derived IF1d7-sup (Fig. 7D). The core protein released into the culture supernatants (IF2d7-, IF2d14-, and IF2d22-sup) of HCVcc-infected ORL8c cells was persistently detected, although at somewhat lower levels than in the RSc cells (Fig. 7E). The level of intracellular HCV RNA in the ORL8c cells was $>10^7$ copies/μg total RNA at IF2d14; this is also somewhat lower than in the RSc cells (Fig. 7F). However, RT-PCR analysis revealed that the expression levels of HCV entry factors (CD81, SR-BI, Claudin-1, and Occuldin) were comparable among HuH-7, RSc, Li23, ORL8c, and ORL11c cells (Fig. 7G). Immunofluorescence analysis showed that the staining levels of dsRNA and HCV proteins were also comparable between HCVcc-infected ORL8c and RSc cells (IF2d7) (Fig. 7H). Colocalization of lipid droplet and HCV core protein was also observed in HCVcc-infected ORL8c and RSc cells (Supplemental Fig. 5), as previously reported (Miyanari et al., 2007). In summary, we demonstrated that ORL8c cells persistently supported the HCV life cycle.

4. Discussion

In this study, we found that human hepatoma Li23-derived cells possess the environments needed for robust genome-length HCV RNA replication and persistent production of infectious HCV. Using Li23-derived cell lines, we developed subgenomic and genome-length HCV RNA replication systems, drug assay systems, and a persistent HCV production system, which correspond to the counterparts of those using HuH-7-derived cell lines (Supplemental Table 2). It is noteworthy that the ORL8c cells cured from ORL8 cells, which were selected by the indicator of HCV RNA replication, showed good potential for producing HCV-JFH1. This finding suggests that the host factors required for robust HCV RNA replication – rather than those for HCV infection or reformation – are key determinants for reproducing the HCV life cycle in cell culture. In fact, we observed similar expression levels of the HCV entry factors between Li23- and HuH-7-derived cells. Therefore, such host factors might be commonly expressed in both ORL8c and RSc cells (Ariumi et al., 2007, 2008; Kuroki et al., 2009).

Our microarray analysis clearly demonstrated that OL8 and OL11 cell lines established in this study were not of HuH-7 cell origin, and revealed that Li23-derived cells possessed rather different expression profiles from those in HuH-7-derived cells (Fig. 3B), although similar liver-specific gene expression profiles were observed in both cell lineages (Fig. 3A). In addition, this analysis revealed that at least OL8 and OL11 cells possessed characteristic expression profiles of the parental Li23 cells, as Oc and OAc cells also showed the HuH-7-type expression profile. Therefore, further comparative studies on the mechanism(s) of HCV proliferation using Li23- and HuH-7-derived cell lines (e.g. ORL8c vs. RSc) may identify new host factor(s) required for efficient HCV proliferation.

A specific combination of adaptive mutations (Q1112R, K1609E, and S2200R) (Abe et al., 2007) is also a key determinant with which to find the Li23 cell line. Until the finding of such a combination of adaptive mutations, we had failed to establish any non-HuH-7-derived cells harboring the HCV replicon. Although it remains unclear what mechanism underlies these adaptive mutations that enhance HCV RNA replication, these mutations might be useful for the development HCV RNA replication systems of various HCV strains.

ORL8 and ORL11 assay systems might become important tools for evaluating or screening anti-HCV reagents, because these assay systems were frequently more sensitive to anti-HCV reagents than the HuH-7-derived OR6 assay system. However, the fact that the ORL8 and ORL11 assays were each more sensitive than the OR6 assay may be due to the fact that OR6 has a higher level of HCV RNA replication than ORL8 and ORL11 cells. Recently, we developed HCV replicon reporter assay systems using four genotype 1b HCV strains (1B-4, KAH5, O, and 1B-5), and found diverse sensitivities against various anti-HCV reagents among the replicons (Nishimura et al., 2009). In that study, we demonstrated that the sensitivities to anti-HCV reagents were not dependent on the replication levels of HCV RNA, and suggested that factor(s) other than the HCV RNA level are involved in conferring sensitivities to anti-HCV reagents including IFN-α (Nishimura et al., 2009). Therefore, the practical use of HuH-7- and Li23-derived assay systems would be very effective for accurately evaluating anti-HCV activity.

Finally, the most important feature of this report is that we were able to persistently produce infectious HCVcc using ORL8c cells. ORL8c-produced HCVcc would be very useful not only for verification of data obtained from HuH-7-derived cells but also for obtaining a variety of new information about the HCV life cycle.

Acknowledgments

We thank Takashi Nakamura and Atsumi Morishita for their technical assistance. We also thank S. Hirohashi, M. Namba, and D. Trono for Li21, Li24, OUMS29, IHH10.3, and IHH12 cell lines. This

work was supported by a grant-in-aid for research on hepatitis from the Ministry of Health, Labor and Welfare of Japan.

Appendix A. Supplementary data

Supplementary data associated with this article can be found, in the online version, at doi:10.1016/j.virusres.2009.08.006.

References

Abe, K., Ikeda, M., Dansako, H., Naka, K., Kato, N., 2007. Cell culture-adaptive NS3 mutations required for the robust replication of genome-length hepatitis C virus RNA. Virus Res. 125, 88–97.

Ali, S., Pellerin, C., Lamarre, D., Kukolj, G., 2004. Hepatitis C virus subgenomic replicons in the human embryonic kidney 293 cell line. J. Virol. 78, 491–501.

Ariumi, Y., Kuroki, M., Abe, K., Dansako, H., Ikeda, M., Wakita, T., Kato, N., 2007. DDX3 DEAD-box RNA helicase is required for hepatitis C virus RNA replication. J. Virol. 81, 13922–13926.

Ariumi, Y., Kuroki, M., Dansako, H., Abe, K., Ikeda, M., Wakita, T., Kato, N., 2008. The DNA damage sensors, ataxia-telangiectasia mutated kinase and checkpoint kinase 2 are required for hepatitis C virus RNA replication. J. Virol. 82, 9639–9646.

Bartenschlager, R., Sparacio, S., 2007. Hepatitis C virus molecular clones and their replication capacity in vivo and in cell culture. Virus Res. 127, 195–207.

Blight, K.J., McKeating, J.A., Rice, C.M., 2002. Highly permissive cell lines for subgenomic and genomic hepatitis C virus RNA replication. J. Virol. 76, 13001–13014.

Burlone, M.E., Budkowska, A., 2009. Hepatitis C virus cell entry: role of lipoproteins and cellular receptors. J. Gen. Virol. 90, 1055–1070.

Chevaliez, S., Pawlotsky, J.M., 2007. Interferon-based therapy of hepatitis C. Adv. Drug Deliv. Rev. 59, 1222–1241.

Choo, Q.L., Kuo, G., Weiner, A.J., Overby, L.R., Bradley, D.W., Houghton, M., 1989. Isolation of a cDNA clone derived from a blood-borne non-A, non-B viral hepatitis genome. Science 244, 359–362.

Dansako, H., Naganuma, A., Nakamura, T., Ikeda, F., Nozaki, A., Kato, N., 2003. Differential activation of interferon-inducible genes by hepatitis C virus core protein mediated by the interferon stimulated response element. Virus Res. 97, 17–30.

Date, T., Kato, T., Miyamoto, M., Zhao, Z., Yasui, K., Mizokami, M., Wakita, T., 2004. Genotype 2a hepatitis C virus subgenomic replicon can replicate in HepG2 and IMY-N9 cells. J. Biol. Chem. 279, 22371–22376.

Gottwein, J.M., Bukh, J., 2008. Cutting the gordian knot-development and biological relevance of hepatitis C virus cell culture systems. Adv. Virus Res. 71, 51–133.

Hadziyannis, S.J., Sette H.Jr., Morgan, T.R., Balan, V., Diago, M., Marcellin, P., Ramadori, G., Bodenheimer H.Jr., Bernstein, D., Rizzetto, M., Zeuzem, S., Pockros, P.J., Lin, A., Ackrill, A.M., 2004. Peginterferon-alpha2a and ribavirin combination therapy in chronic hepatitis C: a randomized study of treatment duration and ribavirin dose. Ann. Intern. Med. 140, 346–355.

Hijikata, M., Kato, N., Ootsuyama, Y., Nakagawa, M., Shimotohno, K., 1991. Gene mapping of the putative structural region of the hepatitis C virus genome by in vitro processing analysis. Proc. Natl. Acad. Sci. U.S.A. 88, 5547–5551.

Hijikata, M., Mizushima, H., Tanji, Y., Komoda, Y., Hirowatari, Y., Akagi, T., Kato, N., Kimura, K., Shimotohno, K., 1993. Proteolytic processing and membrane association of putative nonstructural proteins of hepatitis C virus. Proc. Natl. Acad. Sci. U.S.A. 90, 10773–10777.

Ikeda, M., Abe, K., Dansako, H., Nakamura, T., Naka, K., Kato, N., 2005. Efficient replication of a full-length hepatitis C virus genome, strain O, in cell culture, and development of a luciferase reporter system. Biochem. Biophys. Res. Commun. 329, 1350–1359.

Ikeda, M., Abe, K., Yamada, M., Dansako, H., Naka, K., Kato, N., 2006. Different anti-HCV profiles of statins and their potential for combination therapy with interferon. Hepatology 44, 117–125.

Ikeda, M., Kato, N., 2007. Modulation of host metabolism as a target of new antivirals. Adv. Drug Deliv. Rev. 59, 1277–1289.

Ikeda, M., Sugiyama, K., Mizutani, T., Tanaka, T., Tanaka, K., Sekihara, H., Shimotohno, K., Kato, N., 1998. Human hepatocyte clonal cell lines that support persistent replication of hepatitis C virus. Virus Res. 56, 157–167.

Ikeda, M., Yi, M., Li, K., Lemon, S.M., 2002. Selectable subgenomic and genome-length dicistronic RNAs derived from an infectious molecular clone of the HCV-N strain of hepatitis C virus replicate efficiently in cultured Huh7 cells. J. Virol. 76, 2997–3006.

Kato, N., Hijikata, M., Ootsuyama, Y., Nakagawa, M., Ohkoshi, S., Sugimura, T., Shimotohno, K., 1990. Molecular cloning of the human hepatitis C virus genome from Japanese patients with non-A, non-B hepatitis. Proc. Natl. Acad. Sci. U.S.A. 87, 9524–9528.

Kato, N., Nakazawa, T., Mizutani, T., Shimotohno, K., 1995. Susceptibility of human T-lymphotropic virus type 1 infected cell line MT-2 to hepatitis C virus infection. Biochem. Biophys. Res. Commun. 206, 863–869.

Kato, N., Shimotohno, K., 2000. Systems to culture hepatitis C virus. Curr. Top. Microbiol. Immunol. 242, 261–278.

Kato, N., Sugiyama, K., Namba, K., Dansako, H., Nakamura, T., Takami, M., Naka, K., Nozaki, A., Shimotohno, K., 2003a. Establishment of a hepatitis C virus subgenomic replicon derived from human hepatocytes infected in vitro. Biochem. Biophys. Res. Commun. 306, 756–766.

Kato, T., Date, T., Miyamoto, M., Furusaka, A., Tokushige, K., Mizokami, M., Wakita, T., 2003b. Efficient replication of the genotype 2a hepatitis C virus subgenomic replicon. Gastroenterology 125, 1808–1817.

Kishine, H., Sugiyama, K., Hijikata, M., Kato, N., Takahashi, H., Noshi, T., Nio, Y., Hosaka, M., Miyanari, Y., Shimotohno, K., 2002. Subgenomic replicon derived from a cell line infected with the hepatitis C virus. Biochem. Biophys. Res. Commun. 293, 993–999.

Kuroki, M., Ariumi, Y., Ikeda, M., Dansako, H., Wakita, T., Kato, N., 2009. Arsenic trioxide inhibits hepatitis C virus RNA replication through modulation of the glutathione redox system and oxidative stress. J. Virol. 83, 2338–2348.

Lindenbach, B.D., Evans, M.J., Syder, A.J., Wolk, B., Tellinghuisen, T.L., Liu, C.C., Maruyama, T., Hynes, R.O., Burton, D.R., McKeating, J.A., Rice, C.M., 2005. Complete replication of hepatitis C virus in cell culture. Science 309, 623–626.

Lindenbach, B.D., Rice, C.M., 2005. Unravelling hepatitis C virus replication from genome to function. Nature 436, 933–938.

Lohmann, V., Körner, F., Koch, J., Herian, U., Theilmann, L., Bartenschlager, R., 1999. Replication of subgenomic hepatitis C virus RNAs in a hepatoma cell line. Science 285, 110–113.

Matto, M., Rice, C.M., Aroeti, B., Glenn, J.S., 2004. Hepatitis C virus core protein associates with detergent-resistant membranes distinct from classical plasma membrane rafts. J. Virol. 78, 12047–12053.

Miyanari, Y., Atsuzawa, K., Usuda, N., Watashi, K., Hishiki, T., Zayas, M., Bartenschlager, R., Wakita, T., Hijikata, M., Shimotohno, K., 2007. The lipid droplet is an important organelle for hepatitis C virus production. Nat. Cell Biol. 9, 1089–1097.

Mori, K., Abe, K., Dansako, H., Ariumi, Y., Ikeda, M., Kato, N., 2008. New efficient replication system with hepatitis C virus genome derived from a patient with acute hepatitis C. Biochem. Biophys. Res. Commun. 371, 104–109.

Moriishi, K., Matsuura, Y., 2007. Evaluation systems for anti-HCV drugs. Adv. Drug Deliv. Rev. 59, 1213–1221.

Murakami, K., Kimura, T., Osaki, M., Ishii, K., Miyamura, T., Suzuki, T., Wakita, T., Shoji, I., 2008. Virological characterization of the hepatitis C virus JFH-1 strain in lymphocytic cell lines. J. Gen. Virol. 89, 1587–1592.

Nishimura, G., Ikeda, M., Mori, K., Nakazawa, T., Ariumi, Y., Dansako, H., Kato, N., 2009. Replicons from genotype 1b HCV-positive sera exhibit diverse sensitivities to anti-HCV reagents. Antiviral Res. 82, 42–50.

Pietschmann, T., Lohmann, V., Kaul, A., Krieger, N., Rinck, G., Rutter, G., Strand, D., Bartenschlager, R., 2002. Persistent and transient replication of full-length hepatitis C virus genomes in cell culture. J. Virol. 76, 4008–4021.

Saito, I., Miyamura, T., Ohbayashi, A., Harada, H., Katayama, T., Kikuchi, Y., Watanabe, Y., Koi, S., Onji, M., Ohta, Y., Choo, Q.L., Houghton, M., Kuo, G., 1990. Hepatitis C virus infection is associated with the development of hepatocellular carcinoma. Proc. Natl. Acad. Sci. U.S.A. 87, 6547–6549.

Thomas, D.L., 2000. Hepatitis C epidemiology. Curr. Top. Microbiol. Immunol. 242, 25–41.

Wakita, T., Pietschmann, T., Kato, T., Date, T., Miyamoto, M., Zhao, Z., Murthy, K., Habermann, A., Kräusslich, H.G., Mizokami, M., Bartenschlager, R., Liang, T.J., 2005. Production of infectious hepatitis C virus in tissue culture from a cloned viral genome. Nat. Med. 11, 791–796.

Zhong, J., Gastaminza, P., Cheng, G., Kapadia, S., Kato, T., Burton, D.R., Wieland, S.F., Uprichard, S.L., Wakita, T., Chisari, F.V., 2005. Robust hepatitis C virus infection in vitro. Proc. Natl. Acad. Sci. U.S.A. 102, 9294–9299.

Zhu, H., Dong, H., Eksioglu, E., Hemming, A., Cao, M., Crawford, J.M., Nelson, D.R., Liu, C., 2007. Hepatitis C virus triggers apoptosis of a newly developed hepatoma cell line through antiviral defense system. Gastroenterology 133, 1649–1659.

Zhu, Q., Guo, J.T., Seeger, C., 2003. Replication of hepatitis C virus subgenomes in nonhepatic epithelial and mouse hepatoma cells. J. Virol. 77, 9204–9210.

J Gastroenterol (2009) 44:856–863
DOI 10.1007/s00535-009-0075-1

ORIGINAL ARTICLE—LIVER, PANCREAS, AND BILIARY TRACT

Interferon-α-induced mTOR activation is an anti-hepatitis C virus signal via the phosphatidylinositol 3-kinase-Akt-independent pathway

Azusa Matsumoto · Tatsuki Ichikawa · Kazuhiko Nakao · Hisamitsu Miyaaki · Kumi Hirano · Masumi Fujimito · Motohisa Akiyama · Satoshi Miuma · Eisuke Ozawa · Hidetaka Shibata · Shigeyuki Takeshita · Hironori Yamasaki · Masanori Ikeda · Nobuyuki Kato · Katsumi Eguchi

Received: 28 July 2008 / Accepted: 14 April 2009 / Published online: 13 May 2009

Abstract
Object The interferon-induced Jak-STAT signal alone is not sufficient to explain all the biological effects of IFN. The PI3-K pathways have emerged as a critical additional component of IFN-induced signaling. This study attempted to clarify that relationship between IFN-induced PI3-K-Akt-mTOR activity and anti-viral action.
Result When the human normal hepatocyte derived cell line was treated with rapamycin (rapa) before accretion of IFN-α, tyrosine phosphorylation of STAT-1 was diminished. Pretreatment of rapa had an inhibitory effect on the IFN-α-induced expression of PKR and p48 in a dose dependent manner. Rapa inhibited the IFN-α inducible IFN-stimulated regulatory element luciferase activity in a dose-dependent manner. However, wortmannin, LY294002 and Akt inhibitor did not influence IFN-α inducible luciferase activity. To examine the effect of PI3-K-Akt-mTOR on the anti-HCV action of IFN-α, the full-length HCV replication system, OR6 cells were used. The pretreatment of rapa attenuated its anti-HCV replication effect in comparison to IFN-α alone, whereas the pretreatment with PI3-K inhibitors, wortmannin and LY294002 and Akt inhibitor did not influence IFN-induced anti-HCV replication.
Conclusion IFN-induced mTOR activity, independent of PI3K and Akt, is the critical factor for its anti-HCV activity. Jak independent mTOR activity involved STAT-1 phosphorylation and nuclear location, and then PKR is expressed in hepatocytes.

Keywords mTOR · STAT-1 · Interferon · HCV · PKR

Abbreviations

IFN	Interferon
HCV	Hepatitis C virus
STAT	Signal transducers and activators of transcription
ISGF-3	IFN-stimulated gene factor 3
ISRE	IFN-stimulated regulatory element
PKR	Double-stranded RNA-dependent protein kinase
Rapa	Rapamycin
PI3-K	Phosphatidylinositol 3-kinase
mTOR	Mammalian target of rapamycin
siRNA	Small interfering RNA

Introduction

Currently, a chronic hepatitis C virus (HCV) infection is the major cause of hepatocellular carcinoma worldwide [1]. Therefore, an anti-HCV strategy is important for prevention of carcinogenesis. Advancement in the treatment of HCV by a combination of pegylated interferon (IFN) and

A. Matsumoto · K. Hirano
Department of Clinical Pharmaceutics,
Graduate School of Biomedical Sciences,
Nagasaki University, Nagasaki, Japan

T. Ichikawa (✉) · K. Nakao · H. Miyaaki · M. Fujimito · M. Akiyama · S. Miuma · E. Ozawa · H. Shibata · S. Takeshita · K. Eguchi
The First Department of Internal Medicine,
Graduate School of Biomedical Sciences, Nagasaki University,
1-7-1 Sakamoto, Nagasaki 852-8501, Japan
e-mail: ichikawa@net.nagasaki-u.ac.jp

H. Yamasaki
Health Research Center, Graduate School of Biomedical Sciences, Nagasaki University, Nagasaki, Japan

M. Ikeda · N. Kato
Department of Molecular Biology, Graduate School of Medicine and Dentistry, Okayama University, Okayama, Japan

ribavirin is effective in 80% of HCV genotype 2 or 3 cases, but less than 50% of genotype 1 cases. To ameliorate the salvage rate of HCV infection, new anti-HCV agents have been developed to inhibit the life cycle of HCV and are combined with IFN-α [2]. Since IFN-α is the most basic agent for HCV treatment, it is necessary to improvement the salvage rate of HCV infection by clarifying the efficacy of IFN treatment.

The factors associated with a refractory response to IFN treatment are the HCV genotype, viral load, age, sex, fibrosis of the infected liver and metabolic factors such as insulin resistance and steatosis [3]. Increased hepatic expression of the suppressor of cytokine signaling (SOCS) family, known as the Jak-STAT signal inhibitors, especially SOCS-3, is associated with non-response to IFN treatment [4, 5]. It is thought that inflammatory cytokines, such as, interleukin 6, induced by HCV infection can induce SOCS-3 in hepatocyte [5]. SOCS-3 inhibits IFN-induced tyrosine phosphorylation of Jak, then intra-hepatocyte IFN signal transduction is inhibited. For HCV survival, Jak1, Tyk2 and STAT-1,-2 signaling, which is the essential pathway for type 1 IFN-induced anti-viral activity, becomes the attack targets from HCV. The relative lack of a viral response to IFN treatment is associated with blunted IFN signaling [6]. HCV coding proteins also inhibit STAT-1 tyrosine phosphorylation [7]. The cause of a refractory response to IFN treatment is thought to be HCV-induced Jak-STAT signal inhibition.

Type 1 IFN is a pleiotropic cytokine which activates various intra-cellular signal pathways other than the Jak-STAT signal [8]. Additional signaling pathways could either collaborate with STATs at the promoter level and contribute to the activation of the STATs plus transcription factor genes or function totally independent of any STAT factors, thus leading to the activation of transcription factor only genes [8]. The Jak-STAT signal alone is not sufficient to explain all the biological effects of type 1 IFN. The PI3-K and p38 kinase pathways have emerged as critical additional component of IFN-induced signaling [8–10]. p38, activated via IL-1β is enhanced STAT-1 tyrosine phosphorylation and express the anti-viral protein, PKR [9]. The IFN-induced PI3-K-Akt pathway has Jak independent activation, and it is the critical signal for cell survival and insulin action [10], but its relationship with the anti-viral action and PI3-K-Akt pathway is still unclear.

Recently, mTOR, a downstream kinase of PI3-K-Akt pathway, was shown to play a critical role in protein synthesis and anti-viral effects. Kaur and his colleagues [11] reported that the IFN activated mTOR pathway exhibits important regulatory effects in the generation of the IFN responses, including the anti-encephalo myocarditis virus effect. The IFN-induced mTOR is LY294002 sensitive and does not affect the IFN-stimulated regulatory element (ISRE) dependent promoter gene activity. Human cytomegalovirus is inhibited by 5′-AMP-activted protein kinase mediated inhibition of mTOR kinase [12]. In contrast, vesicular stomatitis virus is mTOR dependent [13]. A relationship has been reported between the replication of hepatitis virus and mTOR activity. p21-activated kinase 1 is activated through the mTOR/p70 S6 kinase pathway and regulates the replication of HCV [14]. mTOR activation is dependent upon the PI3-K-Akt and ERK pathways. Gao and colleagues reported that HCV-NS5A protein activates the PI3-K-Akt-mTOR pathway and could inhibit HBV RNA transcription and reduce HBV DNA replication in HepG2 cells [15]. The activation of the N-Ras-PI3-K-Akt-mTOR pathway by HCV is required for cell survival and HCV replication [16]. Therefore, PI3-K, Akt and mTOR activated by HCV are inhibitory signals of HCV replication and survival signals of HCV infected cells. Furthermore, the PI3-K-Akt-mTOR pathway, which is activated by HCV, is thought to be one mechanism for chronic HCV infection [14–16]. However, type 1 IFN-induced PI3-K, Akt and mTOR have not yet been fully evaluated regarding their influence on HCV replication.

This study investigated whether IFN-α induced the PI3-K-Akt-mTOR pathway, whether the Jak-STAT pathway has a relationship with the PI3-K-Akt-mTOR pathway, and, finally, whether IFN induced signal transduction, other than the Jak-STAT pathway, is associated with the anti-HCV activity.

Materials and methods

Reagents and cell culture

Recombinant human IFN-α2b was a generous gift from Schering-Plough KK (Tokyo, Japan). Wortmannin, LY 294002, Akt inhibitor and rapamycin were purchased from Calbiochem (La Jolla, CA, USA). Hc human hepatocyte cells (Applied Cell Biology Research Institute, Kirkland, WA, USA) and HuH-7 human hepatoma cells (American Type Culture Collection, Rockville, MD, USA) were maintained in a chemically defined medium, CS-C completed (Cell Systems, Kirkland, WA, USA) and RPMI (Invitrogen, Grand Island, NY, USA), respectively, supplemented with 5% fetal bovine serum. In the pretreatment of rapamycin and chemical inhibitors for 3 h, the cells were

cultured in 5% RPMI, and then exchanged the medium and treated the cells with IFN-α2b at the indicated time.

Cell viability assay

The cells were measured using the colorimetric cell viability assay method. Cell viability was determined by the colorimetric method using a Cell Counting kit (Wako Life Science, Osaka, Japan). The absorbance of each well was measured at 405 nm with a microtiter plate reader (Multiskan JX, Thermo BioAnalysis Co., Japan). After 2 days of 100 IU/mL IFN-α and 1000 nmol/L rapamycin treatment, Cell viability is expressed as a percentage of the viability in standard media without IFN-α and rapamycin. Data were expressed as the mean ± standard deviation (SD). Statistical significance was assessed using Student's t test. Statistical difference was defined as $P < 0.05$. All numerical results were reported as the mean of four independent experiments.

Western blotting and antibodies

Western blotting with anti-PKR, anti-STAT-1 (Santa Cruz Biotechnology, Santa Cruz, CA, USA), anti-tyrosine-701 phosphorylated STAT-1, anti-serine-727 phosphorylated STAT-1, anti-p48, anti-serine-437 phosphorylated Akt, anti-threonin-308 phosphorylated anti-Akt, anti-Akt, anti-serine-2448 phosphorylated mTOR, anti-serine-2481 phosphorylated mTOR, anti-mTOR, anti-JAK-1 or anti-tyrosine 1022/1023 JAK-1 (Cell Signaling, Beverly, MA, USA) was performed as described previously [9]. Briefly, Hc cells were lysed by the addition of a lysis buffer (50 mmol/L Tris–HCl, pH 7.4, 1% Np40, 0.25% sodium deoxycholate, 0.02% sodium azide, 0.1% SDS, 150 mmol/L NaCl, 1 mmol/L EDTA, 1 mmol/L PMSF, 1 μg/mL each of aprotinin, leupeptin and pepstatin, 1 mmol/L sodium o-vanadate and 1 mmol/L NaF). The samples were separated by electrophoresis on 8–12% SDS polyacrylamide gels and electrotransferred to nitrocellulose membranes, and then blotted with each antibody. The membranes were incubated with horseradish peroxidase-conjugated anti-rabbit IgG or anti-mouse IgG, and the immunoreactive bands were visualized using the ECL chemiluminescence system (Amersham Life Science, Buckinghamshire, England).

Fluorescence immunohistochemistry

The Hc cells were seeded onto 11-mm glass cover-slips in 24-well plates at 2.4×10^5 cells/well. The next day, the medium was replaced with serum-free medium, and the cells were pretreated with 10 or 100 nmol/L rapamycin, or vehicle, for 3 h and then stimulated with 100 IU/mL IFN-α for 10 min. Fluorescence immunohistochemistry was performed as described previously [17]. The cells were incubated with anti-tyrosine-701 phosphorylated STAT1 antibody for 1 h at room temperature, washed three times in PBS, incubated with rhodamine-conjugated donkey anti-rabbit IgG (Jackson ImmunoResearch Laboratories, Inc., West Grove, PA, USA) for 1 h, washed in PBS, and mounted in Vectashield Mounting Medium (Vector Laboratories Inc., Burlingame, CA, USA). Nuclear staining was performed using Hoechst 33258 (Invitrogen Japan K.K., Tokyo, Japan). An immunofluorescence analysis was done using an Olympus BX50 microscope (Tokyo, Japan) and the image was captured by a Nikon DXM 1200 digital camera (Tokyo, Japan).

Reporter gene assay

A pISRE-Luc cis-reporter plasmid containing five copies of the ISRE sequence and the firefly luciferase gene and pRL-SV40 containing the SV40 early enhancer/promoter and the renilla luciferase gene were obtained from Clontech (San Diego, CA, USA) and Promega (Madison, WI, USA), respectively. The HuH-7 cells were grown in 24-well multiplates and transfected with 1 μg of pISRE-Luc and 10 ng of pRL-SV40 as a standard by the lipofection method. One day later, the cells were incubated in the absence or presence of varying concentrations of chemical blockers and IFN-α, and the luciferase activities in the cells were determined using a dual-luciferase reporter assay system and a TD-20/20 luminometer (Promega). The data were expressed as the relative ISRE-luciferase activity.

HCV replicon system

OR6 cells stably harboring the full-length genotype 1 replicon, ORN/C-5B/KE [18], were used to examine the influence of the anti-HCV effect of IFN. The cells were cultured in Dulbecco's modified Eagle's medium (Gibco-BRL, Invitrogen) supplemented with 10% fatal bovine serum, penicillin and streptomycin and maintained in the presence of G418 (300 mg/L; Geneticin, Invitrogen). This replicon was derived from the 1B-2 strain (strain HCV-o, genotype 1b), in which the *Renilla* luciferase gene is introduced as a fusion protein with neomycin to facilitate the monitoring of HCV replication. After the treatment, the cells were harvested with *Renilla* lysis reagent (Promega, Madison, WI, USA) and then were subjected to a luciferase assay according to the manufacturer's protocol. mTOR gene knock down is used siRNA (Cell Signaling). 100 nmol/L mTOR specific and non-targeted siRNA as a control was transfected to OR6 cells in accordance with the appended manual. One day later, the cells were incubated in either the absence or presence of 10 IU/mL IFN-α.

Results

IFN-α-induced activity of STAT-1 is inhibited by rapamycin pretreatment

To attempt to clearly identify the influence of mTOR to IFN-α-induced anti-viral protein expression rapamycin (rapa), the specific inhibitor of mTOR, was added prior to treatment with IFN-α. Hc cells have been used as normal hepatocytes in previous reports [19]. The Hc cells were incubated in the absence or presence of IFN-α with or without pretreatment with rapa for 2 h the cells were then harvested for the Western blot analysis (Fig. 1). IFN-α clearly induced tyrosine and serine phosphorylation of STAT-1 at 5 (Fig. 1a, lane 4) and 10 min (Fig. 1a, lane 6), respectively, in the absence of rapa. However, when the Hc cells were pretreated with rapa before IFN-α stimulation, the levels of tyrosine and serine phosphorylated STAT-1 were clearly and rapidly lower than those induced by IFN-α alone 5 min after treatment in tyrosine (Fig. 1a, lane 5). Jak-1, an upstream protein of STAT-1, was equally phosphorylated by IFN-α with (Fig. 1b, lane3) or without (Fig. 1b, lane2) pretreatment with rapa. The viability of the Hc cells was 1 in vehicle, 0.93±0.21 in IFN-α treatment and 0.88±0.34 in rapamycin treatment. No difference in the cell viability the among vehicle, IFN-α and rapamycin treatment was not recognized in our assay. The viability of the HuH-7 and OR6 cells also demonstrated no difference between the presence of IFN-α and rapamycin treatment and the absence thereof.

IFN inducible gene products are diminished by pretreatment of rapamycin

Since pretreatment with rapa inhibited the IFN-α induced STAT-1 activity, the phosphorylation of tyrosine and serine and nuclear translocation, the effect of pretreated with rapa on the IFN-α inducible gene product was examined. The protein levels of PKR, an anti-viral protein that acts as a mRNA translation inhibiter activated by double stranded RNA [20, 21], and p48, key component of ISGF-3 with activated STAT-1 and -2 [22], were induced by IFN-α treatment for 3 h in Hc cells (Fig. 1c, lanes 1, 2). However, pretreatment with rapa had an inhibitory effect on IFN-α-induced PKR and p48 in a dose dependent manner (Fig. 1c, lanes 2–4).

The serine 473 on Akt and serine 2448 on mTOR are phosphorylated by IFN-α

Because pretreatment with rapa affected the IFN-α signaling (Fig. 1), the ability of IFN-α to activate the Akt-mTOR pathway was investigated. The phosphorylation of serine-2448 residues of mTOR and serine-473 residue of

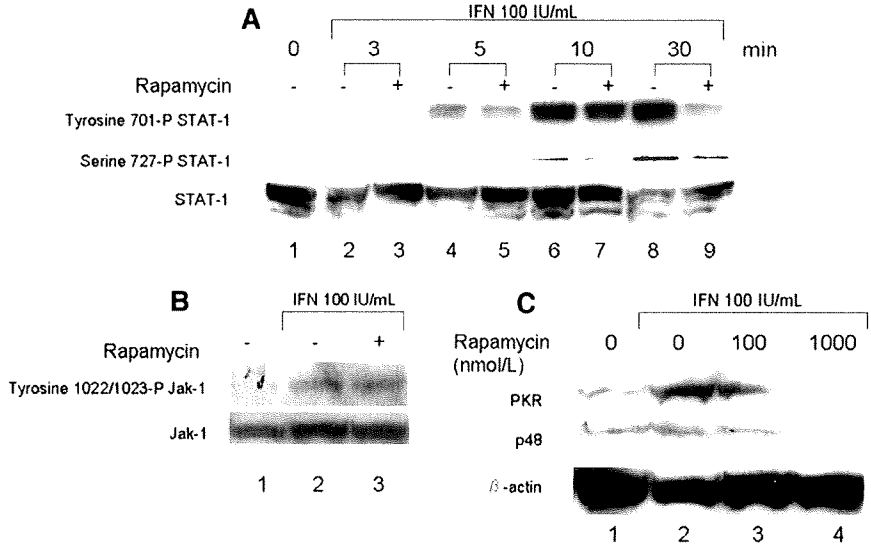

Fig. 1 Alteration in the distribution of IFN-α induced phosphorylated STAT-1 (**a**) and Jak-1 (**b**) by rapamycin and effect of rapamycin on IFN-α-induced PKR and p48 (**c**). Hc cells were pretreated without (*lanes 1, 2, 4, 6,* and *8*) or with 1 μmol/L rapa (*lanes 3, 5, 7,* and *9*). These Hc cells were stimulated by 100 IU/L IFN-α (*lane 2–9*) for 30 min. Phosphorylated STAT-1 at tyrosine-701 residue (*upper panel*) and at serine-727 residue (*lower panel*) were analyzed by Western blotting. **a** After pretreatment of 1000 nmol/L rapa (*lane 3*) for 3 h, Hc cells were untreated (*lane 1*) or treated with 100 IU/mL IFN-α (*lanes 2, 3*) for 3 min, then phosphorylated JAK-1 at tyrosine-1022/1023 residue (*first panel*), expression of JAK-1 (*second panel*) were analyzed by Western blotting (**b**). Hc cells were treated with 100 IU/mL of IFN-α in the absence (*lane 2*) or of the presence of pretreatment (*lane 3, 4*). *Lane 1* was not treated IFN-α and calcineurin inhibitors. One day latter, PKR and p48 was determined by Western blotting (**c**)